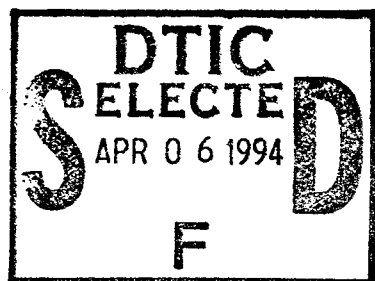


AL/OE-TR-1994-0132



## SEASONAL SONIC BOOM PROPAGATION PREDICTION



W. R. Lundberg

OCCUPATIONAL & ENVIRONMENTAL HEALTH DIRECTORATE  
BIOENVIRONMENTAL ENGINEERING DIVISION  
WRIGHT-PATTERSON AFB OH 45433-7901

MARCH 1994

19950404 149

FINAL REPORT FOR THE PERIOD SEPTEMBER 1991 TO OCTOBER 1992

Approved for public release; distribution is unlimited

AIR FORCE MATERIEL COMMAND  
WRIGHT-PATTERSON AIR FORCE BASE, OHIO 45433-6573

ARMSTRONG  
LABORATORY

19950404 149

## NOTICES

When US Government drawings, specifications, or other data are used for any purpose other than a definitely related Government procurement operation, the Government thereby incurs no responsibility nor any obligation whatsoever, and the fact that the Government may have formulated, furnished, or in any way supplied the said drawings, specifications, or other data, is not to be regarded by implication or otherwise, as in any manner licensing the holder or any other person or corporation, or conveying any rights or permission to manufacture, use, or sell any patented invention that may in any way be related thereto.

Please do not request copies of this report from the Armstrong Laboratory. Additional copies may be purchased from:

National Technical Information Service  
5285 Port Royal Road  
Springfield, Virginia 22161

Federal Government agencies registered with the Defense Technical Information Center should direct requests for copies of this report to:

Defense Technical Information Center  
Cameron Station  
Alexandria, Virginia 22314

## TECHNICAL REVIEW AND APPROVAL

AL/OE-TR-1994 -0132


This report has been reviewed by the Office of Public Affairs (PA) and is releasable to the National Technical Information Service (NTIS). At NTIS, it will be available to the general public, including foreign nations.

This technical report has been reviewed and is approved for publication.



ROBERT C. KULL, JR., MAJ., USAF  
Chief, Noise Effects Branch

FOR THE DIRECTOR



JAMES D. MONTGOMERY, LT COL, USAF, BSC  
Chief  
Bioenvironmental Engineering Division  
Armstrong Laboratory

# REPORT DOCUMENTATION PAGE

Form Approved  
OMB No. 0704-0188

Public reporting burden for this collection of information is estimated to average 1 hour per response, including the time for reviewing instructions, searching existing data sources, gathering and maintaining the data needed, and completing and reviewing the collection of information. Send comments regarding this burden estimate or any other aspect of this collection of information, including suggestions for reducing this burden, to Washington Headquarters Services, Directorate for Information Operations and Reports, 1215 Jefferson Davis Highway, Suite 1204, Arlington, VA 22202-4302, and to the Office of Management and Budget, Paperwork Reduction Project (0704-0188), Washington, DC 20503.

1. AGENCY USE ONLY (Leave blank)		2. REPORT DATE March 1994	3. REPORT TYPE AND DATES COVERED Report September 1991 to October 1992		Final
4. TITLE AND SUBTITLE SEASONAL SONIC BOOM PROPAGATION PREDICTION				5. FUNDING NUMBERS PE: 62202F PR: 7231 TA: 34 WU: 15	
6. AUTHOR(S)  W. R. LUNDBERG					
7. PERFORMING ORGANIZATION NAME(S) AND ADDRESS(ES) Armstrong Laboratory, Occupational & Environmental Health Dir Bioenvironmental Engineering Division Human Systems Center Air Force Materiel Command Wright-Patterson AFB OH 45433-7901				8. PERFORMING ORGANIZATION REPORT NUMBER  AL/OE-TR-1994-0132	
9. SPONSORING / MONITORING AGENCY NAME(S) AND ADDRESS(ES)				10. SPONSORING / MONITORING AGENCY REPORT NUMBER	
11. SUPPLEMENTARY NOTES					
12a. DISTRIBUTION / AVAILABILITY STATEMENT  Approved for public release; distribution is unlimited.				12b. DISTRIBUTION CODE	
13. ABSTRACT (Maximum 200 words)  Seasonal variations in wind and temperature gradients are known to influence the propagation of sonic booms. This report examines predictive techniques in current use which may be refined for application to seasonal Environmental Impact Statements. The effects of seasonally averaged refractive atmospheres on the sonic boom carpet predictions for an example flight of an F-111 at Mach 1.3 and 10,000 feet above Mean Sea Level (MSL) were documented. The effect of such atmospheres on predicted noise exposures due to a real-world mix of supersonic flights was estimated. The example boom environment was chosen to be that near Edwards Air Force Base (EAFB) where sonic booms are known to affect the public. Two distinct atmospheric averaging techniques were applied seasonally and the resulting sonic boom predictions compared to each other and to those predictions obtained using the U.S. Standard Day Atmosphere and the Annual reference Atmosphere for Edwards AFB. The results show the potential benefit of conducting seasonal sonic boom predictions in forecasting the effects which supersonic flight operations have on the public.					
14. SUBJECT TERMS Sonic Boom Environmental Noise Acoustic Propagation				15. NUMBER OF PAGES 59	
				16. PRICE CODE	
17. SECURITY CLASSIFICATION OF REPORT  UNCLASSIFIED	18. SECURITY CLASSIFICATION OF THIS PAGE  UNCLASSIFIED	19. SECURITY CLASSIFICATION OF ABSTRACT  UNCLASSIFIED	20. LIMITATION OF ABSTRACT  UNLIMITED		

THIS PAGE INTENTIONALLY LEFT BLANK

## PREFACE

This study was performed for Armstrong Laboratory at Wright-Patterson Air Force Base, Ohio, under Project/Task 723134, Exploratory Noise and Sonic Boom Research by the Noise Effects Branch, Bioenvironmental Engineering Division.

The author appreciates the technical guidance and support of Mr. Jerry Speakman, retired, and Dr. Ken Plotkin of Wyle Research Laboratories as well as the expertise and programs provided by Dr. Albion Taylor of the National Oceanographic and Atmospheric Administration (NOAA). Final preparation of the report by Ms. Jackie Brennaman and Ms. Bea Heflin is sincerely appreciated.

Accession For		
NTIS	CRA&I	<input checked="checked" type="checkbox"/>
DTIC	TAB	<input type="checkbox"/>
Unannounced		<input type="checkbox"/>
Justification .....		
By .....		
Distribution /		
Availability Codes		
Dist	Avail and/or Special	
A-1		

THIS PAGE INTENTIONALLY LEFT BLANK

## TABLE OF CONTENTS

	Page
Preface .....	iii
Table of Contents .....	v
List of Figures .....	vii
List of Tables .....	ix
INTRODUCTION .....	1
TECHNICAL FORMULATION .....	1
Atmospheric Data .....	1
Operational Data .....	2
PROPAGATION MODELING .....	3
Long-term Exposure Model .....	3
Single-event Overpressure Model .....	4
RESULTS .....	40
Propagation from 10,000 feet .....	40
Propagation from 30,000 feet .....	42
Overpressures at 10,000 feet .....	43
L <sub>Cdn</sub> Contours for 1990 Operational Data .....	44
Comparison of Single-Event to Long-Term Propagation Measures .....	44
CONCLUSIONS .....	46
RECOMMENDATIONS .....	47
REFERENCES .....	48

THIS PAGE INTENTIONALLY LEFT BLANK



## LIST OF FIGURES

Figure	Page
Annual Windless Atmospheres, 10000 ft MSL:	
1. U.S. Standard Day Atm., No Wind .....	5
2. Edwards Range Standard Atm., No Wind .....	6
3. Average Annual Atm. at 0000 Zulu, No Wind .....	7
4. Average Annual Atm. at EAFB, No Wind .....	8
Annual Windy Atmospheres, 10000 ft MSL:	
5. Average Annual Atm. at 0000 Zulu, Eastbound .....	9
6. Average Annual Atm. at 0000 Zulu, Westbound .....	10
7. Average Annual Atm. at EAFB, Eastbound .....	11
8. Average Annual Atm. at EAFB, Westbound .....	12
Winter Atmospheres, 10000 ft MSL:	
9. Average Winter Atm. at 0000 Zulu, Eastbound .....	13
10. Average Winter Atm. at 0000 Zulu, Westbound .....	14
11. Average Winter Atm. at EAFB, Eastbound .....	15
12. Average Winter Atm. at EAFB, Westbound .....	16
Spring Atmospheres, 10000 ft MSL:	
13. Average Spring Atm. at 0000 Zulu, Eastbound .....	17
14. Average Spring Atm. at 0000 Zulu, Westbound .....	18
15. Average Spring Atm. at EAFB, Eastbound .....	19
16. Average Spring Atm. at EAFB, Westbound .....	20
Summer Atmospheres, 10000 ft MSL:	
17. Average Summer Atm. at 0000 Zulu, Eastbound .....	21
18. Average Summer Atm. at 0000 Zulu, Westbound .....	22
19. Average Summer Atm. at EAFB, Eastbound .....	23

20. Average Summer Atm. at EAFB, Westbound .....	24
Fall Atmospheres, 10000 ft MSL:	
21. Average Fall Atm. at 0000 Zulu, Eastbound .....	25
22. Average Fall Atm. at 0000 Zulu, Westbound .....	26
23. Average Fall Atm. at EAFB, Eastbound .....	27
24. Average Fall Atm. at EAFB, Westbound .....	28
Eastbound Flights at 30000 ft MSL:	
25. Average Winter Atm. at EAFB .....	29
26. Average Spring Atm. at EAFB .....	30
27. Average Summer Atm. at EAFB .....	31
28. Average Fall Atm. at EAFB .....	32
29. Edwards Range Standard Atm., No Wind .....	33
L <sub>Cdn</sub> Contours for 1990 operations:	
30. Edwards Range Standard Atm., No Wind .....	34
31. Average Annual Atm. at EAFB .....	35
32. Average Winter Atm. at EAFB .....	36
33. Average Spring Atm. at EAFB .....	37
34. Average Summer Atm. at EAFB .....	38
35. Average Fall Atm. at EAFB .....	39

## LIST OF TABLES

Table	Page
1. Measures of the Predicted Lateral Spread of Sonic Boom for Annual Atmospheres at EAFB Sonic Boom Corridor .....	41
2. Measures of the Predicted Lateral Spread of Sonic Boom for the Regional Average Seasonal Atmospheres at EAFB Sonic Boom Corridor .....	41
3. Measures of the Predicted Lateral Spread of Sonic Boom for the Edwards AFB Range Average Seasonal Atmospheres at EAFB Sonic Boom Corridor ..	41
4. Measures of the Predicted Lateral Spread of Sonic Boom for the Edwards AFB Range Average Seasonal Atmospheres and Standard Atmospheres for an Eastbound Aircraft .....	42
5. Summary of Atmospheric Profile Statistics .....	43
6. Comparison of Single-event to $L_{Cdn}$ Contour Measures of the Asymmetry of Lateral Sonic Boom Propagation .....	45

THIS PAGE INTENTIONALLY LEFT BLANK

## INTRODUCTION

The objective of this study is to assess state-of-the-art methodologies for long-term sonic boom prediction in seasonally varying atmospheres. Existing methods for predicting single-event acoustic propagation in a refractive atmosphere were studied to assess their applicability to and impact on long-term acoustic propagation models in general use. The study was conducted in two parts: (1) a detailed study of single-event carpet boom variations and (2) a study of seasonal changes in cumulative exposure contours. The impact of predicting cumulative exposures on a quarterly basis is assessed. Methods for generating accurate predictions of wind vector gradient refraction are examined for potential application to seasonal sonic boom predictions. A relationship between results obtained using the two methods is established.

A set of typical regional atmospheric profiles and a set of ~2 yr station average atmospheric profiles were used to compare seasonal meteorological databases. The U.S. Standard Day atmosphere and the Edwards Range standard atmosphere were used for comparison of annual exposure predictions. The site chosen for study was the Edwards Air Force Base (EAFB) supersonic flight corridor. The analysis shows the potential benefit of forecasting sonic booms by employing seasonal atmospheric profiles. The single-event forecasts improve the estimation of lateral spreading of sonic booms. Those sonic booms having levels above 1 PSF were documented for study because that is a threshold above which sonic booms are of concern to the community. Long-term forecasts confirmed that the seasonal shifting of the carpet boom evident in the single-event predictions translates effectively into the operational environment.

## TECHNICAL FORMULATION

### Atmospheric Data

The Air Force Flight Test Center's range staff meteorologist provided five atmospheric profiles for this study<sup>1</sup>. The annual and four seasonal profiles were computed from frequent, but not regularly scheduled, rawinsonde launch upper air data averaged over 26 months (4 Nov 89 to 6 Jan 92). The wind speed and directions at each level were computed by averaging the speeds and angular headings at each measured level. A standard deviation of the two measures was available, but not used in this study. These atmospheric profiles were termed EAFB Average profiles in the following discussion.

A previous derivation of regionalized upper air climatology had studied five regions encompassing all 11 southwestern U.S. supersonic MOAs. The work was conducted by the USAF Environmental Technical Applications Center (USAFETAC)<sup>2</sup>. It resulted in regional "average" atmospheric profiles for the year and each season. Here the "average" wind vector at each level was calculated by determining the prevailing (i.e. most frequent) wind direction and the mean scalar wind. The atmospheric profiles were compiled from rawinsonde reporting sites used by the National Weather Service (NWS) and Air Force Air Weather Service at EAFB. Three sites were averaged together in each region, even if there were disparities in site elevation. Such launches are conducted

at 0000 and 1200 Zulu (GMT) time to record diurnal variations and thus cannot reasonably be averaged together. The 0000 Zulu launches correspond to 4-5 PM EAFB time and so were relevant to the common supersonic flight operations in that area. Five out of the total of fifty regional atmospheric profiles were selected accordingly for use in this study. These atmospheric profiles were termed Regional Average atmospheres in the following discussion.

The U.S. Standard Day<sup>3</sup> atmospheric profile is considered to be comparable to annual windless profiles, although it is not explicitly an average of meteorological data. The Edwards Range Standard atmospheric profile was determined from measurements made prior to 1975<sup>4</sup> and does not include wind vector profiles either. The Edwards Range Standard includes Hot and Cold temperature profiles which are offset from the Annual reference profile by a nearly constant amount, and are not considered in this study. Plots of temperature and wind vector profiles are included, where used, beside their respective single-event sonic boom overpressure predictions (Figures 1 through 29).

### Operational Data

Aircraft flight parameters were based on documentation of 1990 supersonic operations in the Black Mountain corridor. Both the full complement of straight-line flights and a representative sample flight were used in separate analyses. In all cases the ground elevation was chosen to be 2316 feet MSL to correspond to the elevation of the Black Mountain operations area. The actual sonic boom carpet would also be altered by changing ground elevation or even local topographical variations. However, the impact of variation in ground level is not a concern of this study.

The actual 1990 supersonic flight operational distribution was used with CORBOOM<sup>5</sup> to provide  $L_{Cdn}$  contours with which an environmental planner will already be familiar. Quarterly predictions were made assuming that 1/4 of the total number of operations occurred in each season. Under this assumption a postulated seasonal reference metric such as  $L_{Cdns}$  is numerically equal to  $L_{Cdn}$ . If all the operations occurred in a given season, then the corresponding contour would actually be an  $L_{Cdn}$  contour and not just its numerical equivalent. The operational dataset was provided as a reference case with the CORBOOM program and was documented for comparison in reference 5. Twelve diving or turning operations were not included because the associated sonic boom propagations would not be symmetric with respect to the East-West flight tracks used most frequently. Such additional boom exposures would render invalid any direct comparison to the predictions of single-event booms generated by East-West flight operations.

A single hypothetical flight was used to produce sonic boom predictions which would characterize the typical 1 PSF carpet widths, shifts and maximum overpressures created by the supersonic operations in the area during each period. Earlier findings<sup>6</sup> have shown that a single flight at the Inverse Root-Mean Inverse Square (IRMIS) altitude of a set of similar flights is representative of the propagated acoustic levels from the

complete set of flight operations. Thus a moderately high (1.3 Mach) airspeed coupled with a moderately low (10 Kft MSL) altitude was selected. The selected flight conditions thereby illustrate the refractive effect and generate a sonic boom which would tend to acoustically dominate the cumulative sonic boom contour. Further simulations of propagation from 30 Kft were conducted to study the upper atmosphere from a more frequently used flight altitude. The F-111 aircraft was chosen because the appropriate Whitman's F-function was included in the Tracing Rays and Aging Pressure Signatures (TRAPS<sup>7</sup>) database. The aircraft's position at the instant of boom generation is fixed at location (0,0) miles in all cases plotted in the figures. Such a "snapshot" of boom propagation from the aircraft at the origin is sufficient to estimate corridor widths and shifting of the sonic boom carpet.

### PROPAGATION MODELING

Two sonic boom prediction models were required to accomplish the objectives of this report. A model which generates carpet-region  $L_{Cdn}$  contours for actual operations distributions in specified atmospheres is required to convey the effects of seasonal variations in the operational environment. A more detailed propagation model is required to illustrate the effects of atmospheric refraction, to compare methods of deriving representative atmospheres and to assess the current limitations of long-term sonic boom exposure prediction methodologies. Both models chosen exercised a ray-tracing approach to calculating propagated acoustic levels. Neither model incorporates calculations of atmospheric absorption. These theoretical constraints limit the conclusions which can be drawn about predictions of overall sonic boom carpet width (geometric cutoff) and the acoustic levels predicted for long ranges. Such constraints are in common use and do not represent a significant limitation in calculations of the effect of the seasonally varying atmosphere.

#### Long-term exposure model

The existing formulation of CORBOOM<sup>5</sup> assumes that the refractive atmosphere has azimuthal symmetry, which is true when only vertical temperature gradients exist. The program uses a temperature profile to determine the sound-speed gradient from which refractive effects are calculated. The asymmetry which results from wind vector gradient refraction was approximated by adjustments to the temperature gradient. The orthogonal (N-S) component of the prevailing wind vector was used to calculate an adjustment to the temperature which would result in an appropriate correction to the sound speed. The formula:

$$T_{adj} = \left[ \frac{20.276\sqrt{T + 273.15} + W_{NS}}{20.276} \right]^2 - 273.15$$

was used, where  $T$  is the seasonally-averaged temperature in °C,  $W_{NS}$  is the orthogonal component of the seasonally-averaged wind vector, and  $T_{adj}$  is the adjusted

temperature at each height in the profile.

For instance, the northbound acoustic rays experience an effectively increased sound speed if the wind component is favorable, whereas the southbound acoustic rays are slowed by the same wind component. CORBOOM does not have a capability to calculate such asymmetric refractive phenomena simultaneously. The asymmetric results were computed separately and the appropriate contours spliced together to produce each seasonal contour prediction. The resulting contours were all plotted at a 1:500000 scale in Figures 30-35. CORBOOM calculates the area within each contour, from which it was easy to estimate the contour's width and lateral shift from the scaled overall length of the contour. These measures were used to assess the potential error occurring each season in comparison to annual windless  $L_{Cdn}$  contour predictions. The CORBOOM predictions were further compared to the contour widths and shifts predicted by a single-event overpressure model to corroborate the use of a single flight for estimation of the relative magnitude of predicted variations.

#### Single-event overpressure model

A PC version of the TRAPS program (TRAPS 89) was used in conjunction with a commercial plotting package to generate ray cone-ground intersection plots. This approach was necessary to work around run-time errors which plagued other methods and for the capability to vary the method used to determine ground impact points. Peak overpressure, in Pascals, at each ray's intersection with the ground could be read from the output files for evaluation. The peak overpressures nearest to the flight centerline, and at 2 (or 6) mile intervals to each side, were read and annotated on the "snapshot" plots in PSF (Figures 1-29). The acoustic ray intercepting the ground nearest to cutoff was included unless it extended beyond the scale of the figures (12 miles), since such rays always produced very low-amplitude booms. Such long-range acoustic signatures are produced only by the ray-theoretic implementation and do not exist in reality. Minor variations in effective Mach number were calculated by TRAPS and tabulated in Tables 1 through 4.

TRAPS allows user-specified increments in Phi (the azimuthal angle of the acoustic ray with respect to a vertical plane through the flight track) to synthesize the ray cone. The Phi increments were chosen to provide accurate sideline predictions, i.e. relatively dense ray-ground impact locations, while reducing computer runtime. Phi increments of  $3^\circ$ ,  $.8^\circ$ ,  $.2^\circ$ ,  $.04^\circ$ ,  $.002^\circ$ , and occasionally  $.0003^\circ$  were used in successive angular regions away from vertical. The furthest two or three incremental angular regions were adjusted for each run to find the calculated geometric cutoff distance within  $\sim .1$  mile. The numerical accuracy of the predicted cutoff width was severely limited by the theoretical constraints of ray-tracing, as mentioned previously. In all cases, the Phi angles were limited within TRAPS by an Admittance Ellipse (see Ref. 7) which was estimated by application of an acoustic version of Snell's Law. All cases in which the Admittance Ellipse limit, or "Snell limit", was reached are annotated in the respective Figures and Tables. This artificially-induced cutoff has been re-examined in more



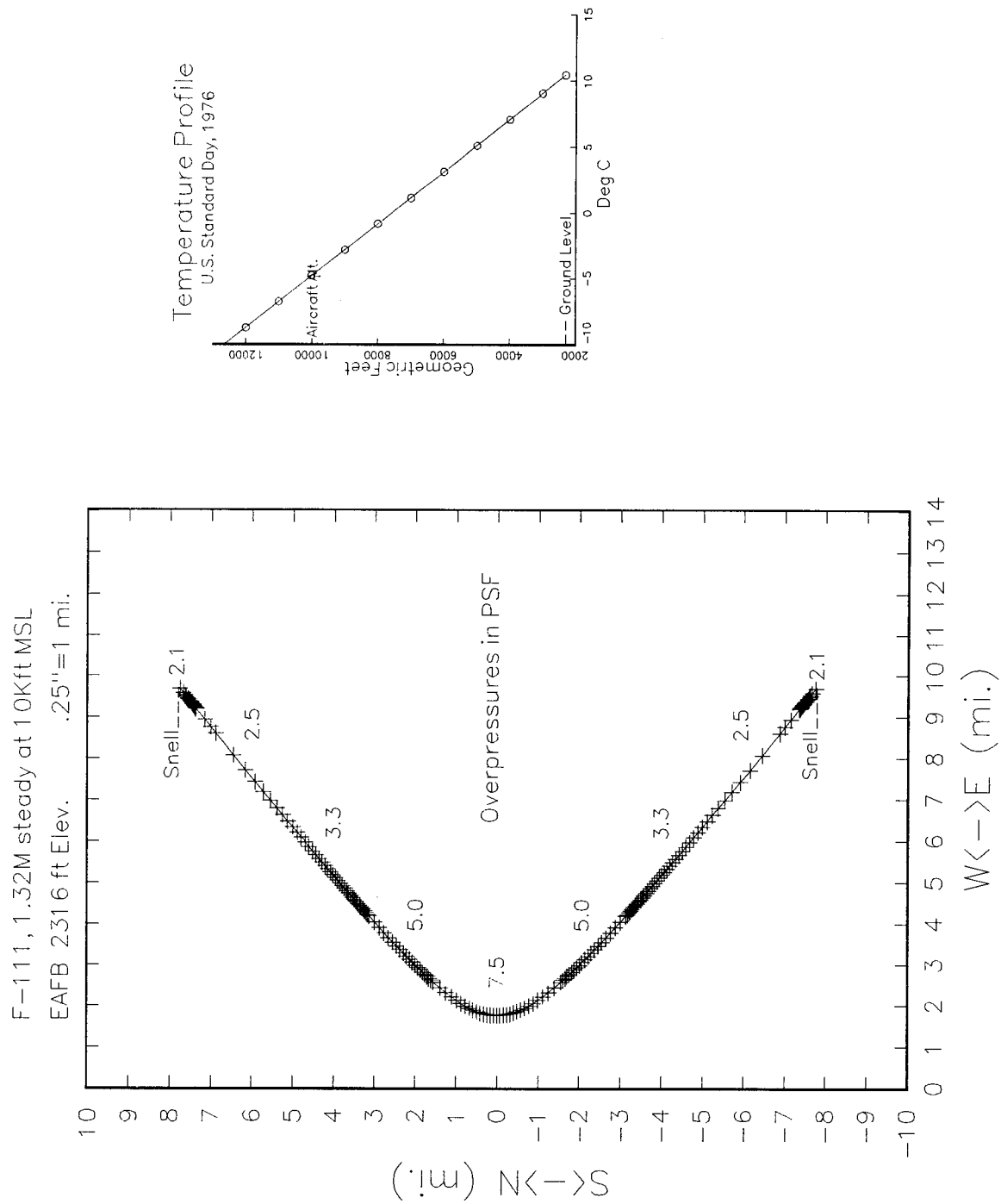


Figure 1. U.S. Standard Day Atmosphere, No Wind

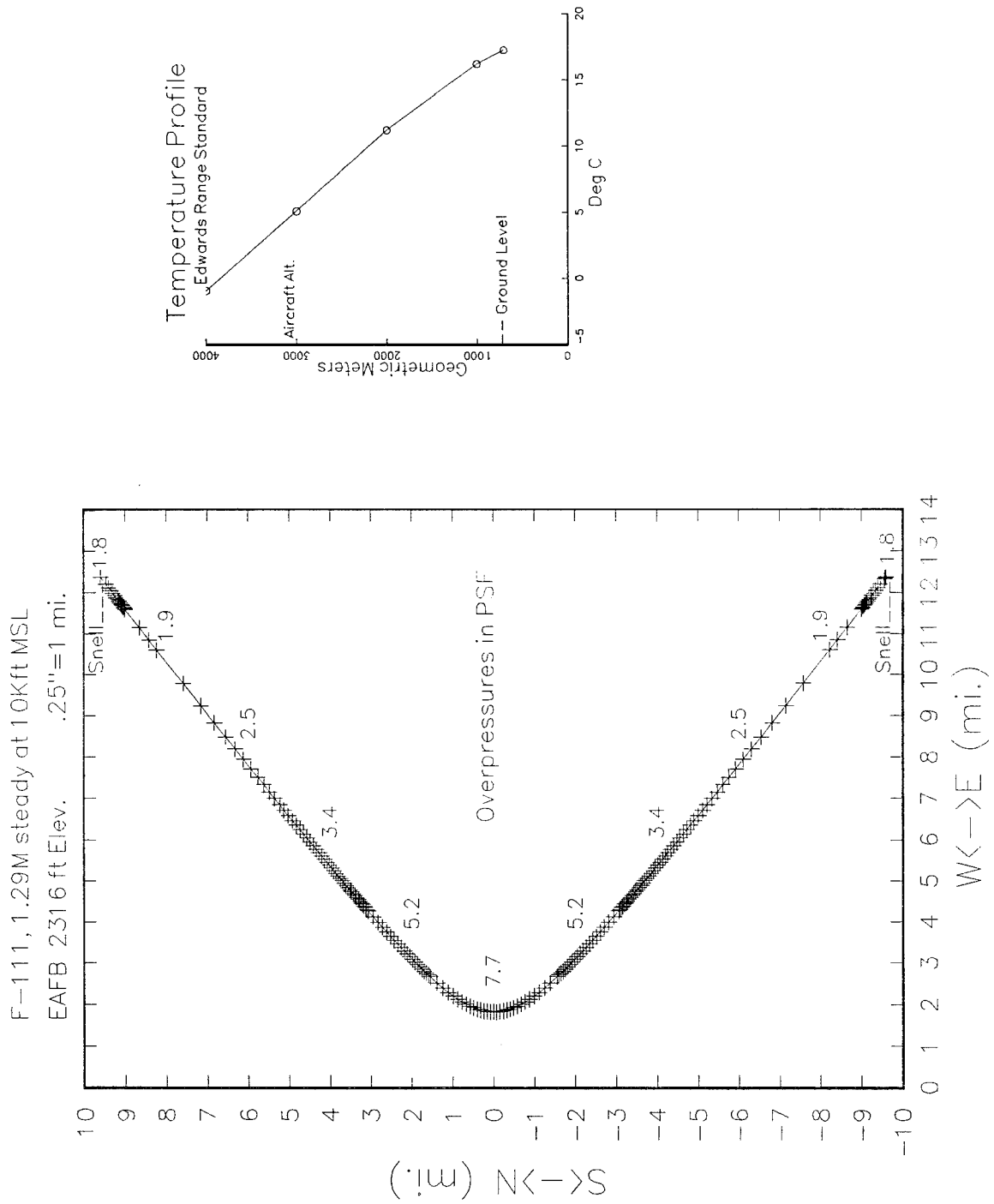


Figure 2. Edwards Range Standard Atmosphere, No Wind

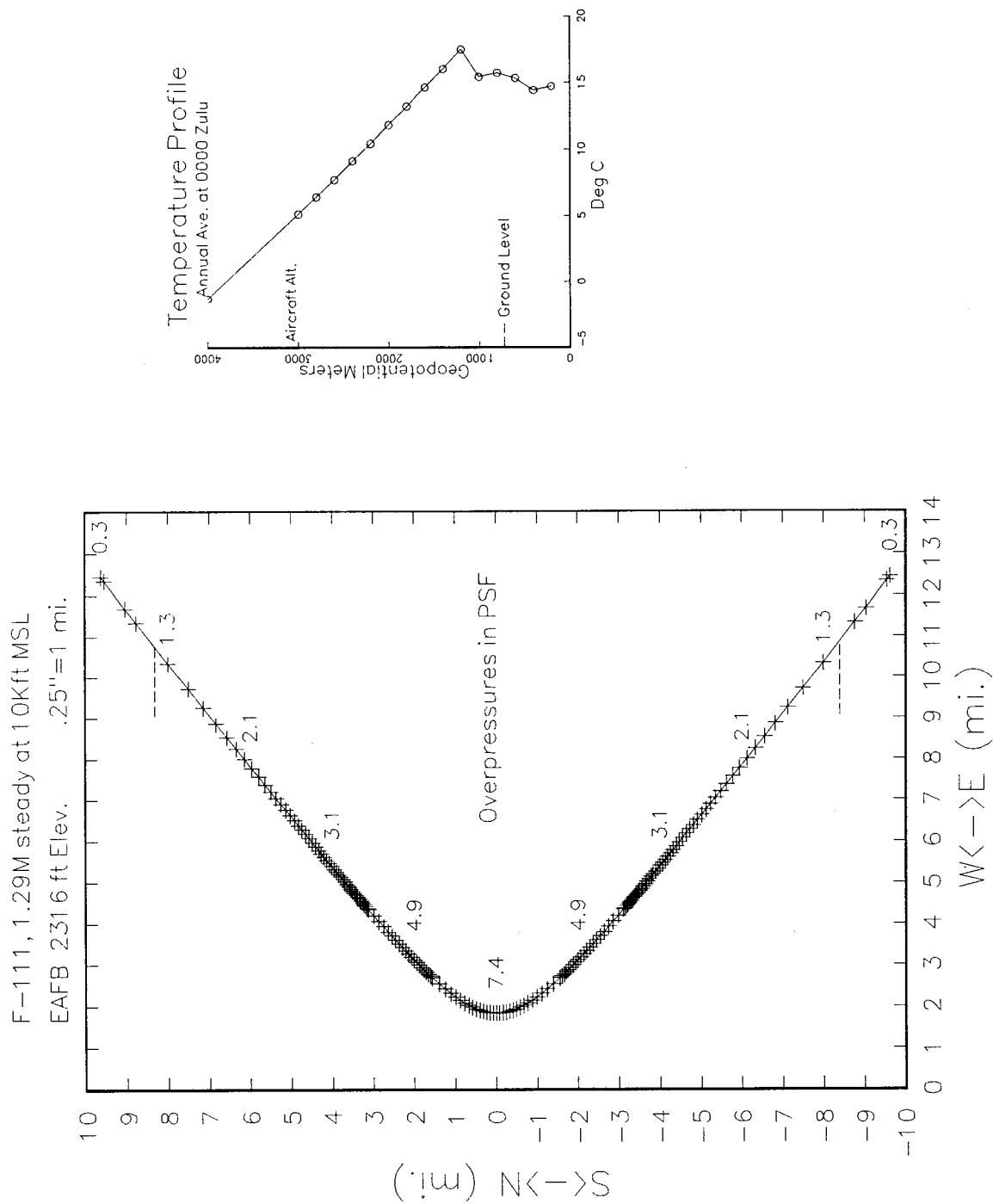


Figure 3. Average Annual Atmosphere at 0000 Zulu, No Wind

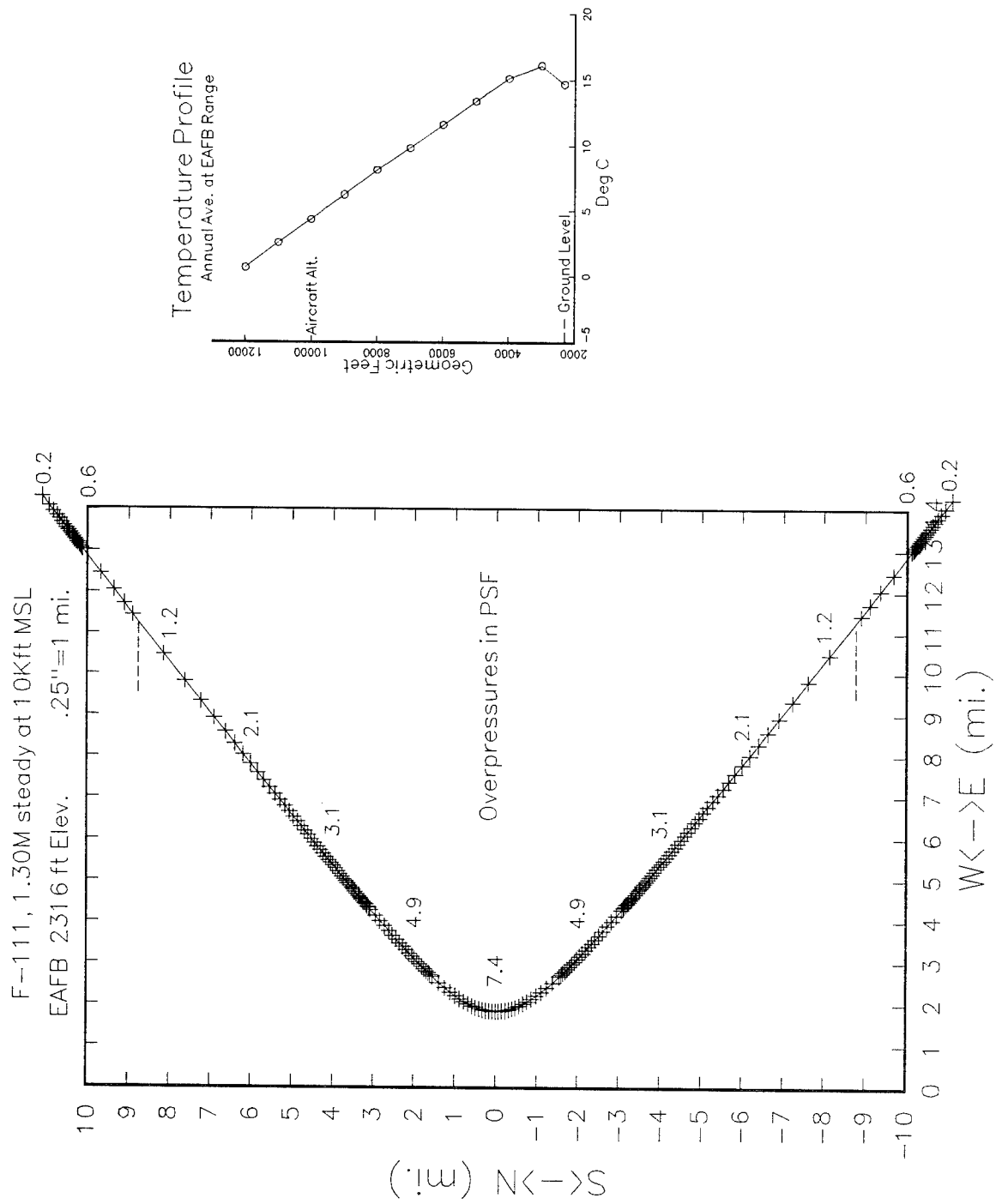


Figure 4. Average Annual Atmosphere at EAFB, No Wind

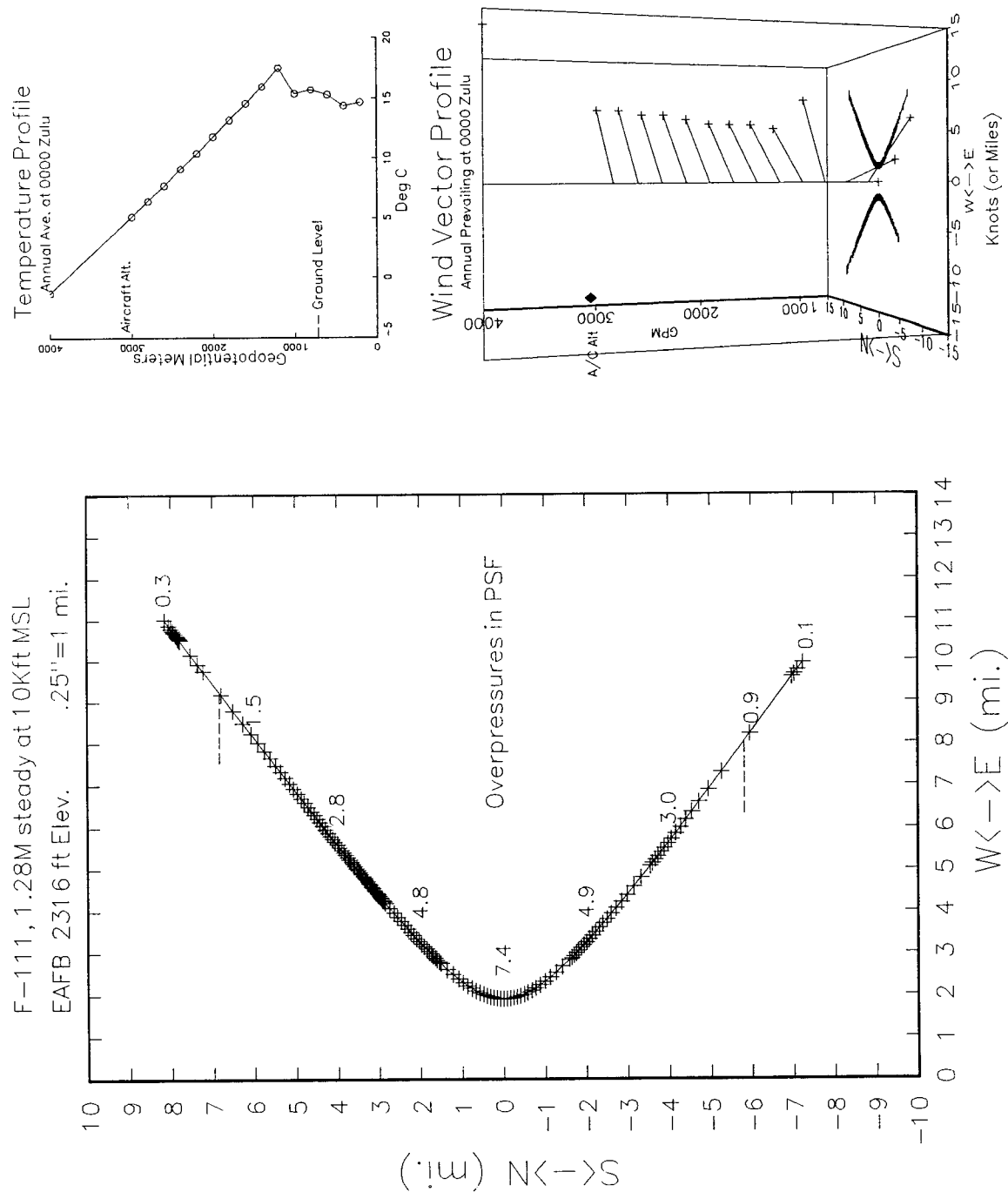


Figure 5. Average Annual Atmosphere at 0000 Zulu, Eastbound

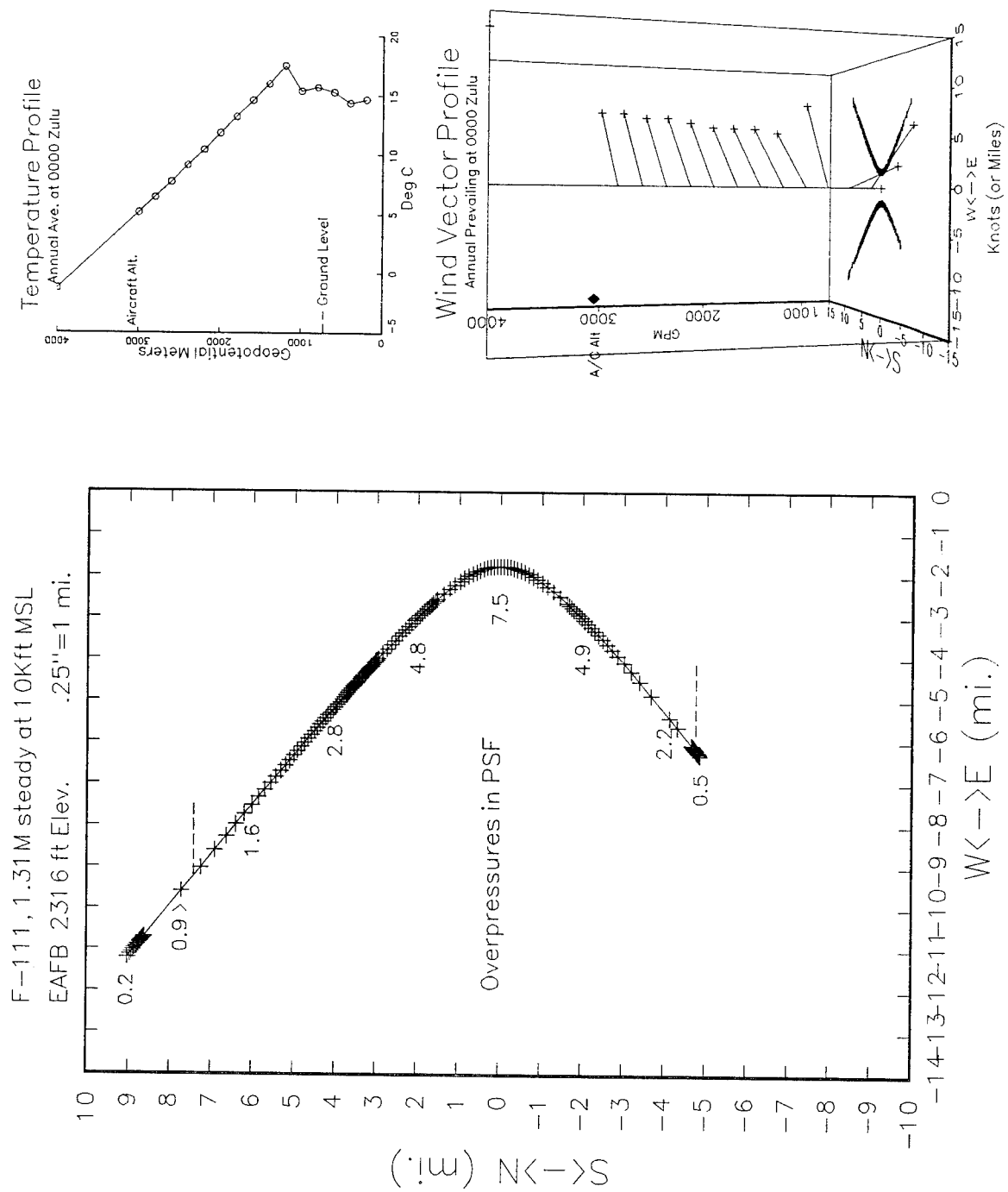


Figure 6. Average Annual Atmosphere at 0000 Zulu, Westbound

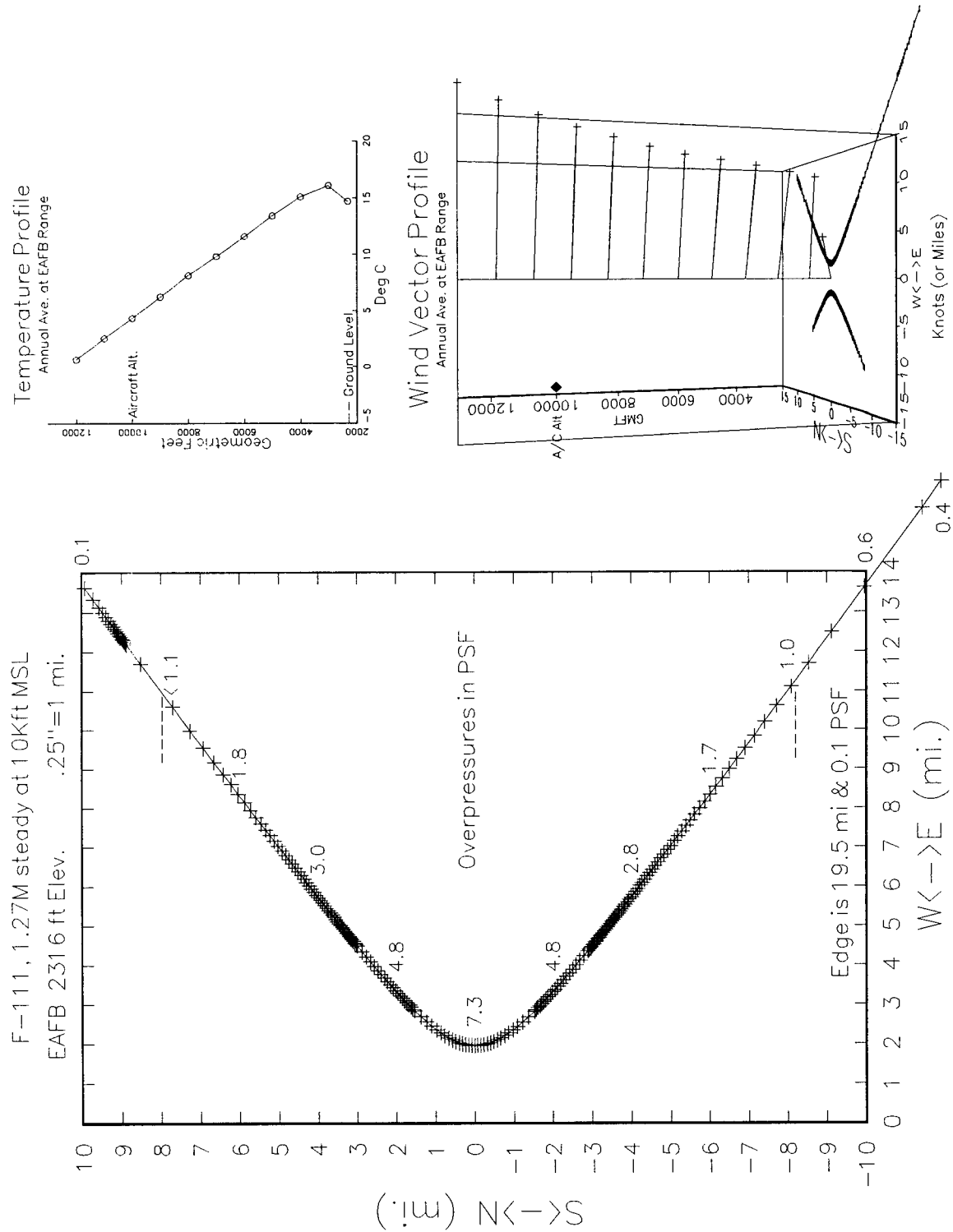


Figure 7. Average Annual Atmosphere at EAFB, Eastbound

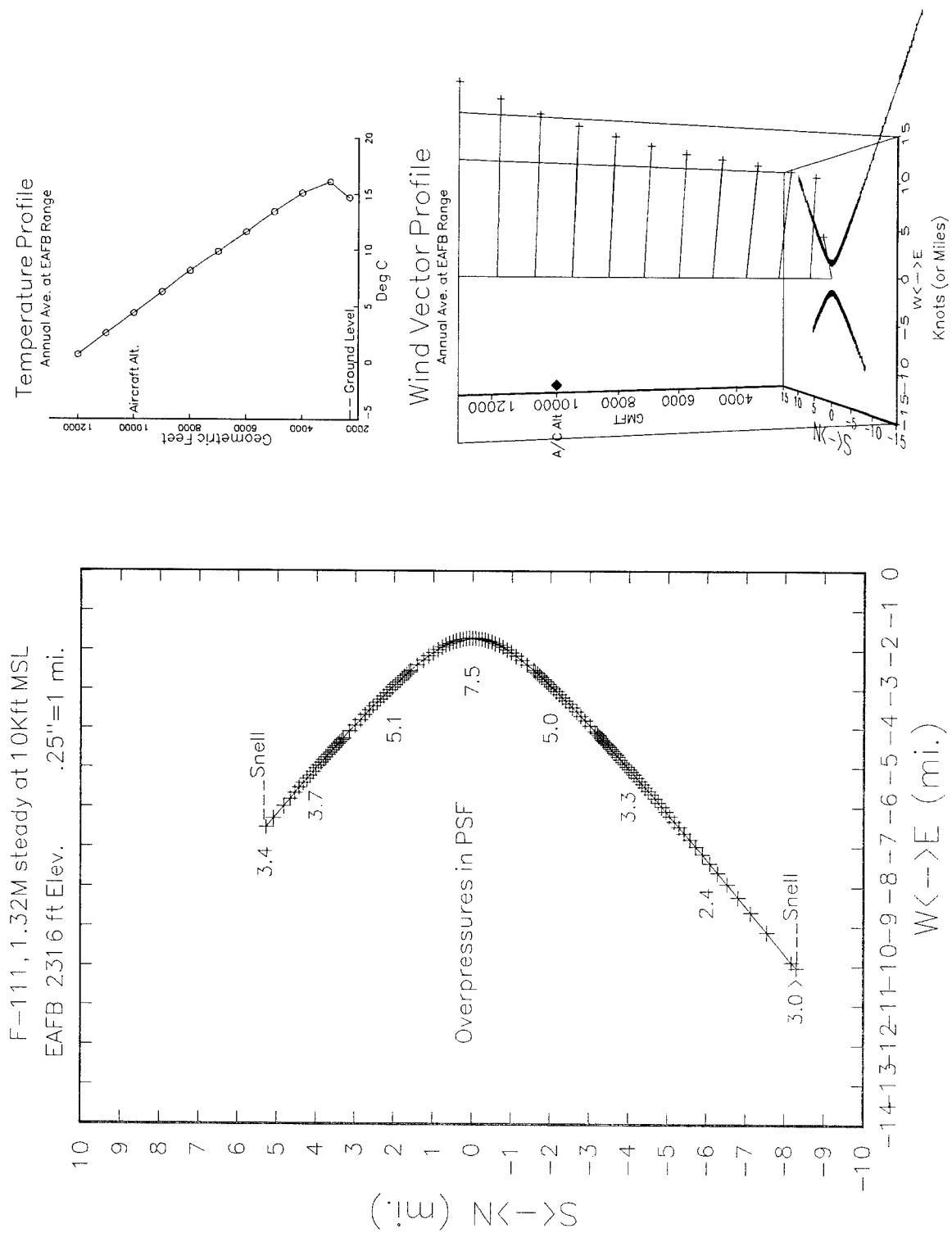


Figure 8. Average Annual Atmosphere at EAFB, Westbound



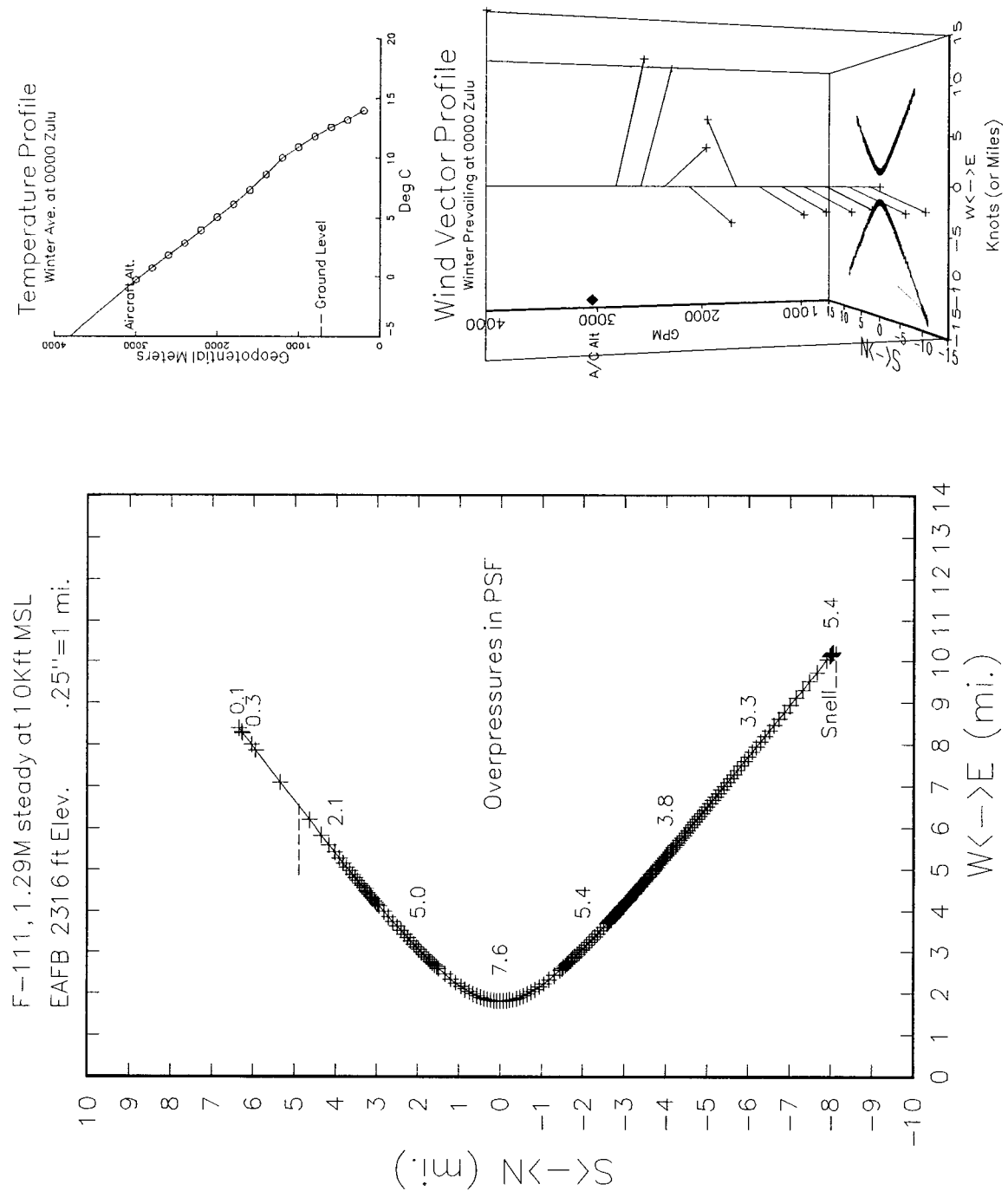


Figure 9. Average Winter Atmosphere at 0000 Zulu, Eastbound

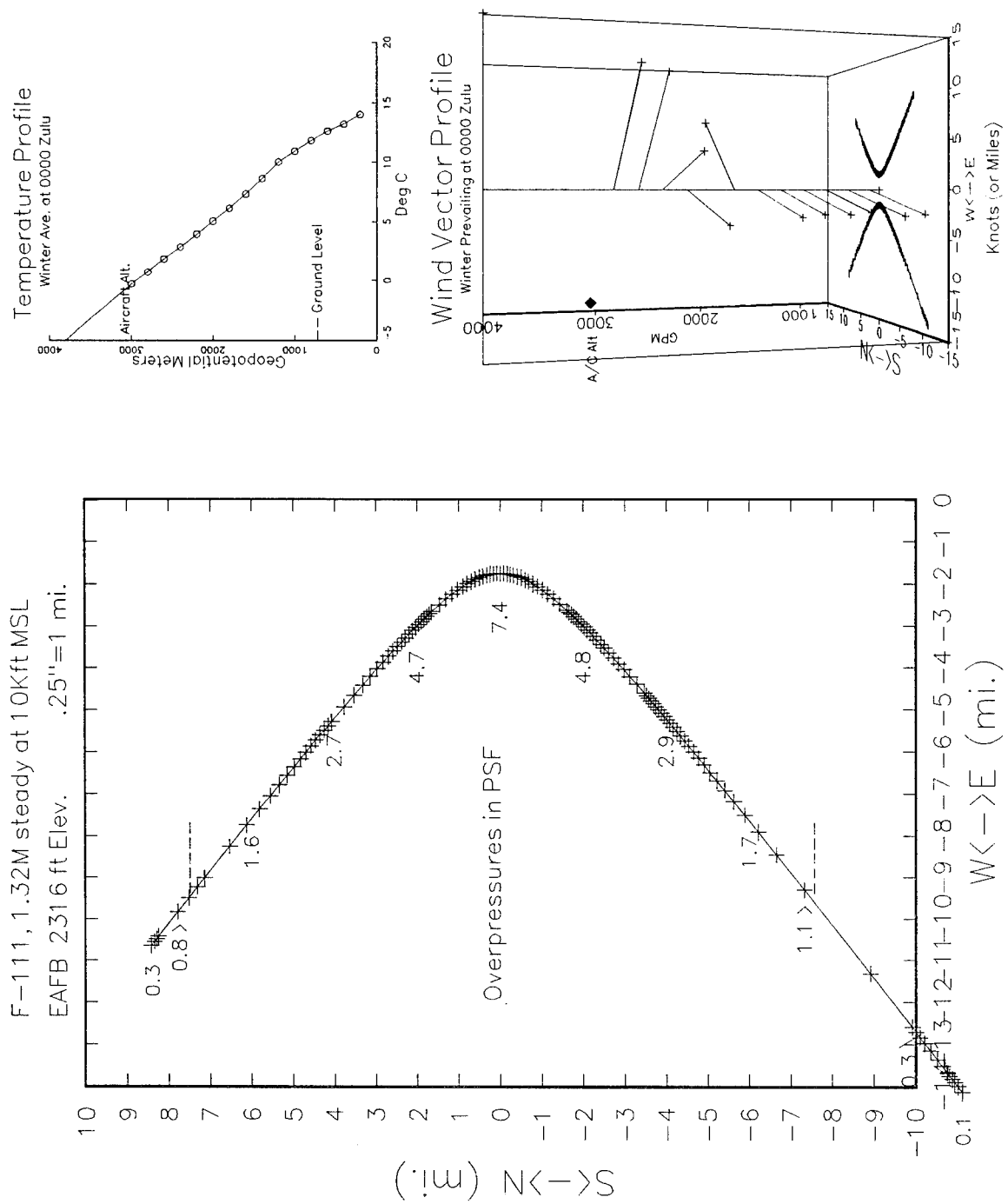


Figure 10. Average Winter Atmosphere at 0000 Zulu, Westbound

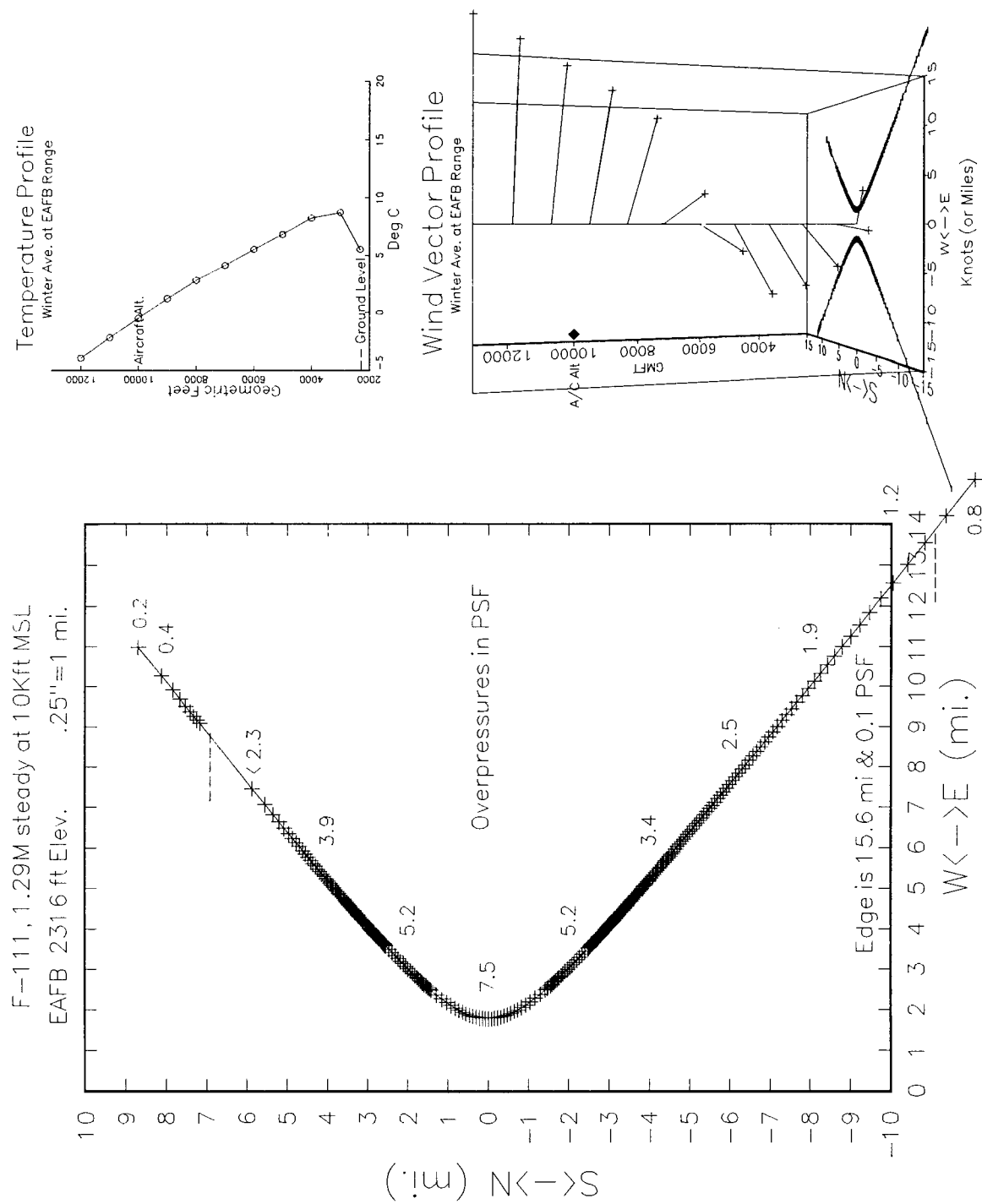


Figure 11. Average Winter Atmosphere at EAFB, Eastbound

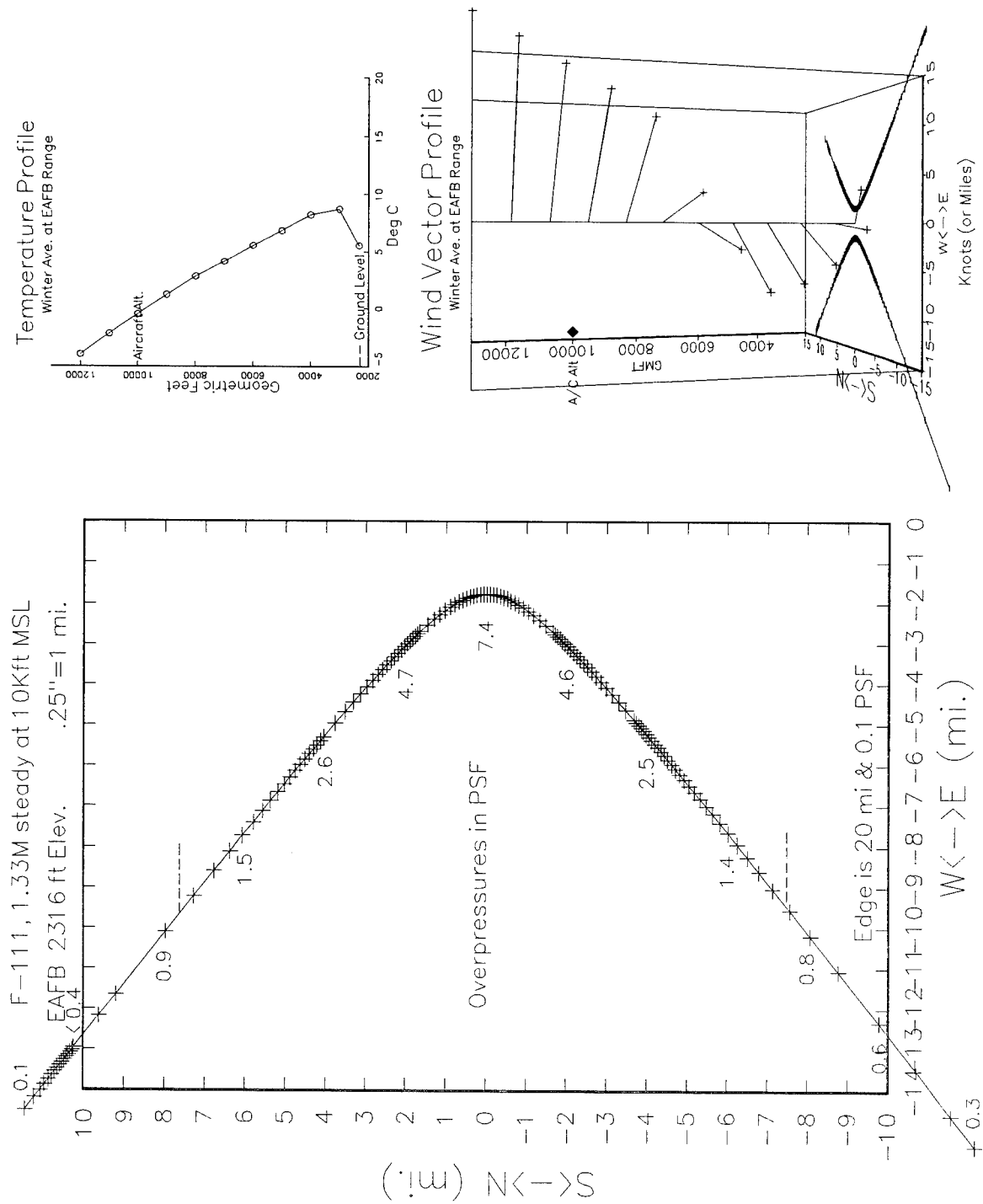


Figure 12. Average Winter Atmosphere at EAFB, Westbound

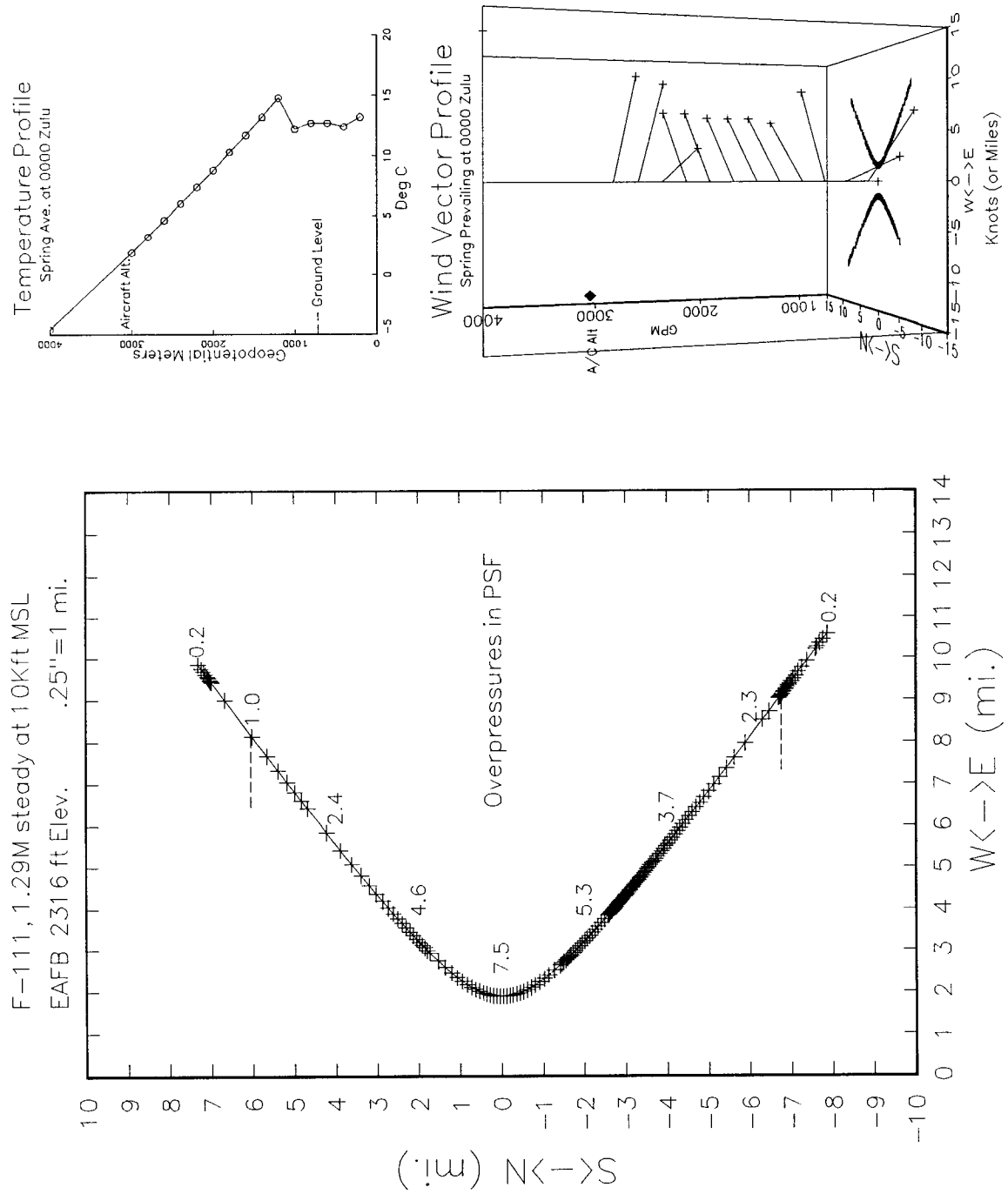


Figure 13. Average Spring Atmosphere at 0000 Zulu, Eastbound

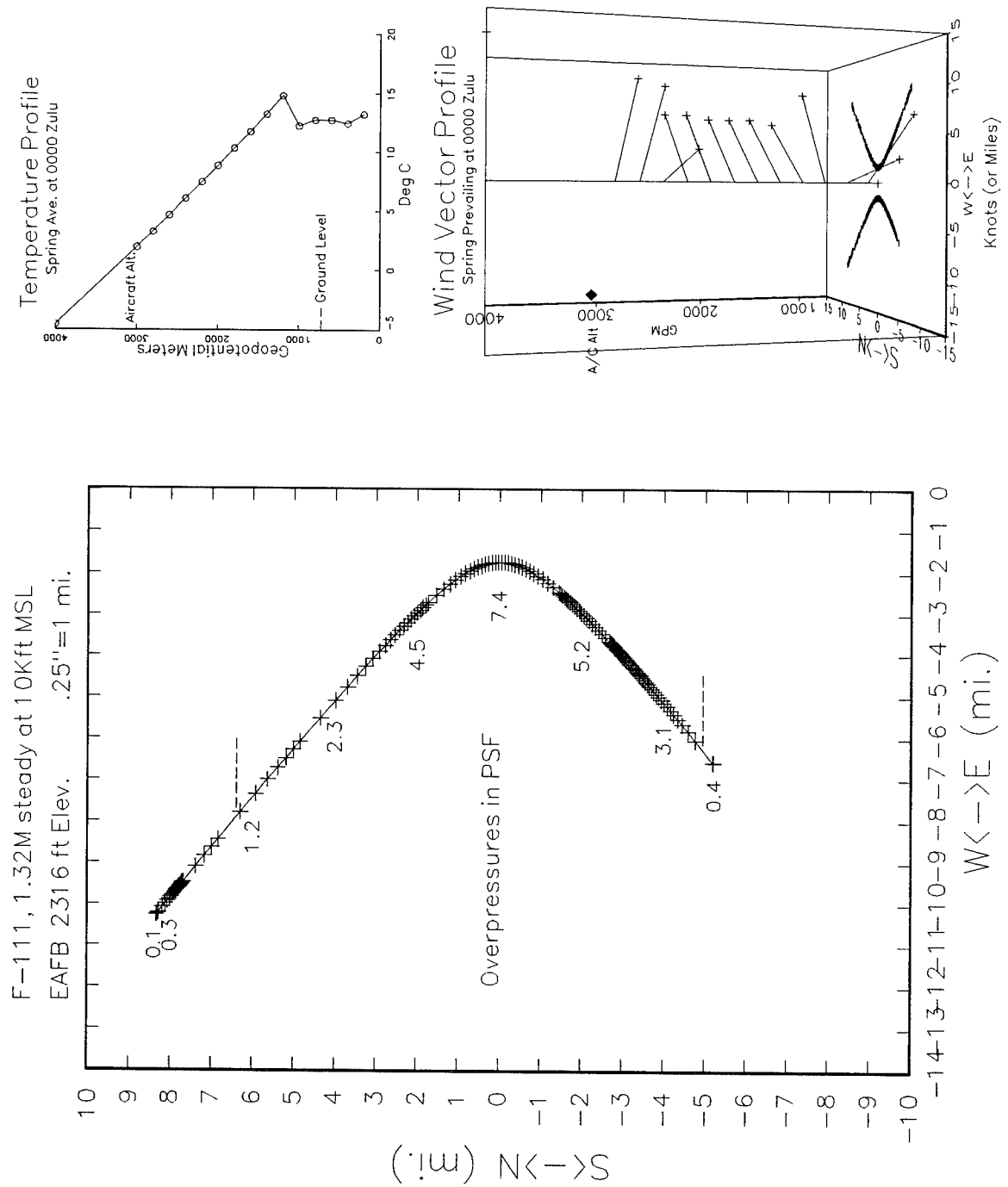


Figure 14. Average Spring Atmosphere at 0000 Zulu, Westbound

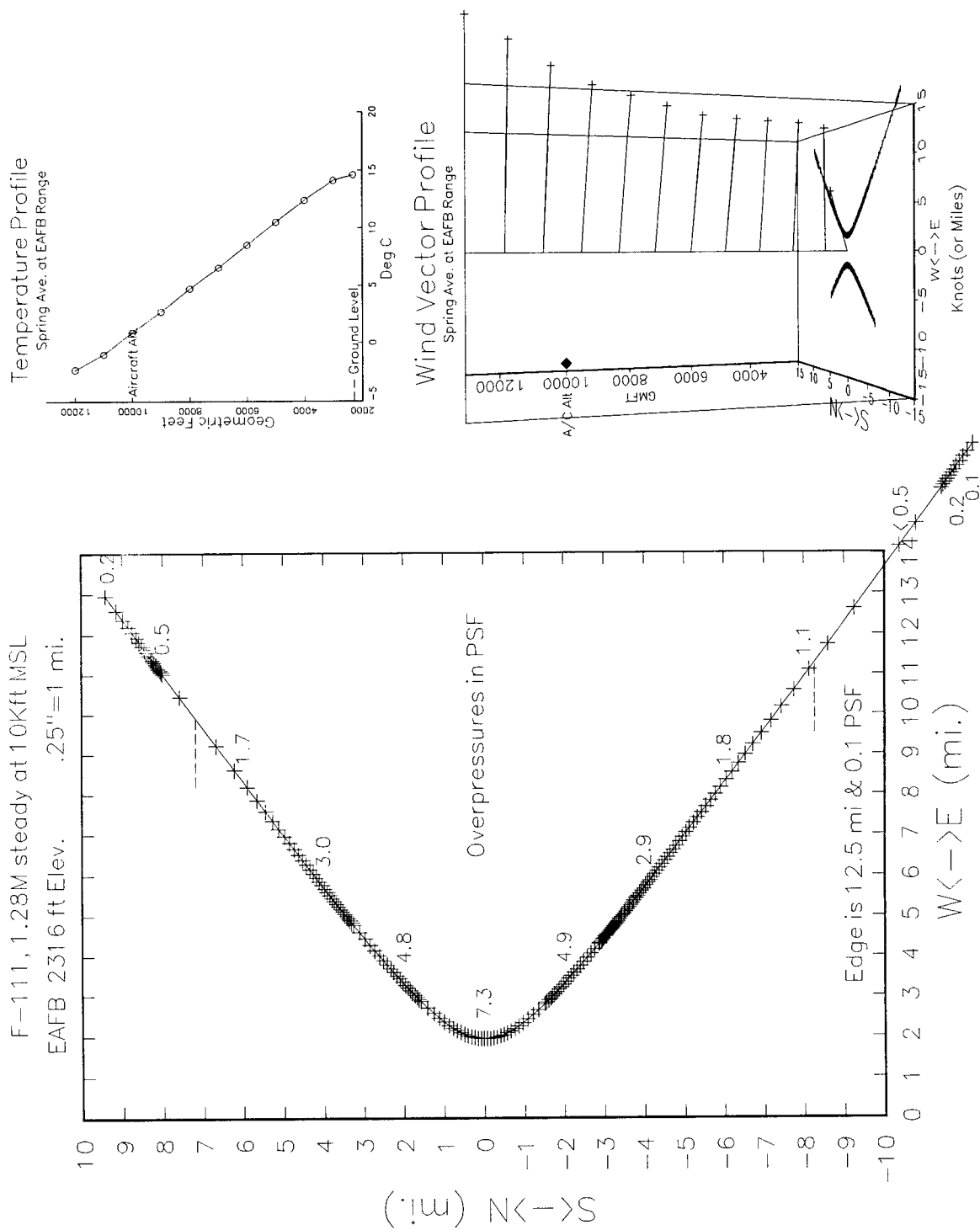


Figure 15. Average Spring Atmosphere at EAFB, Eastbound

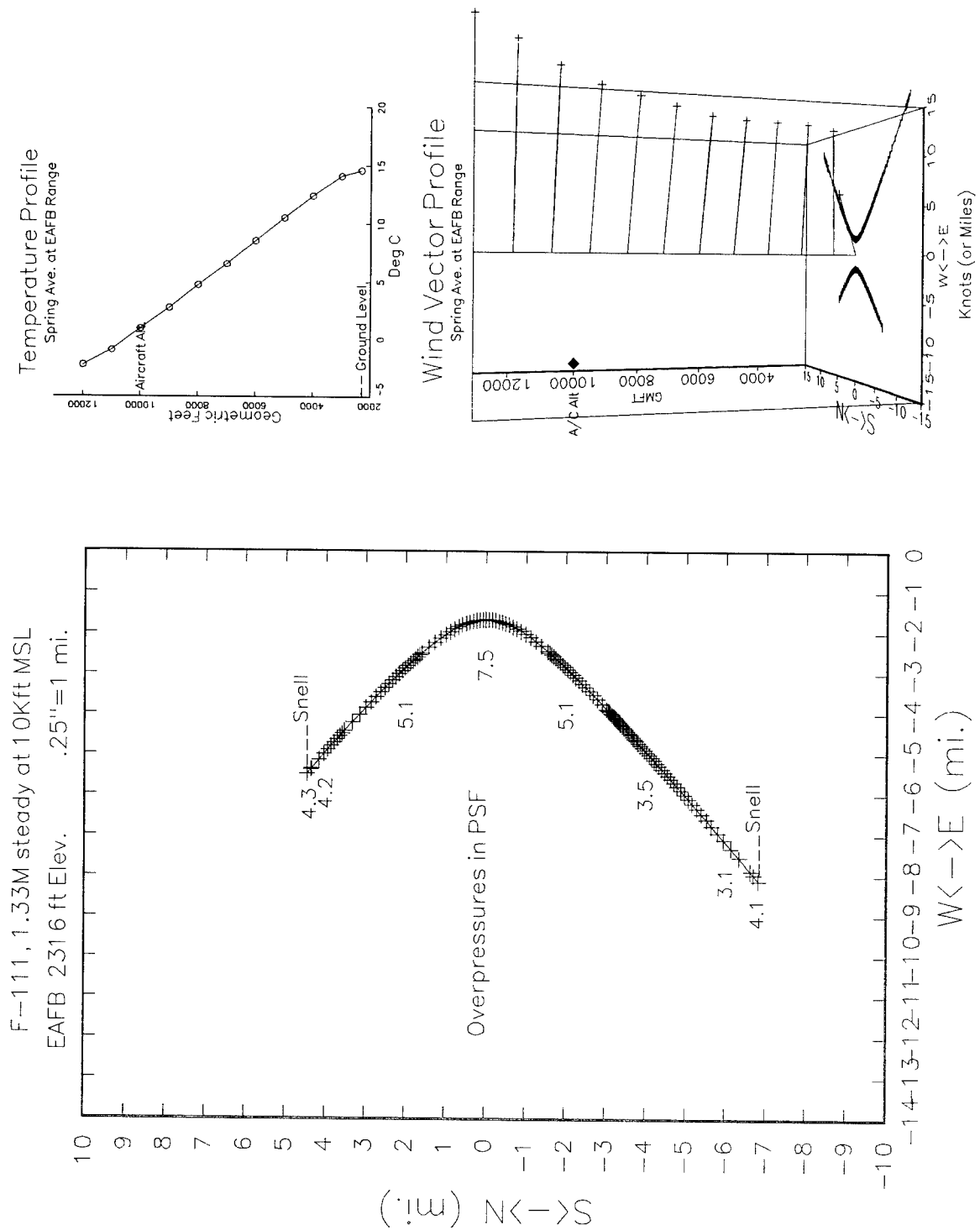


Figure 16. Average Spring Atmosphere at EAFB, Westbound



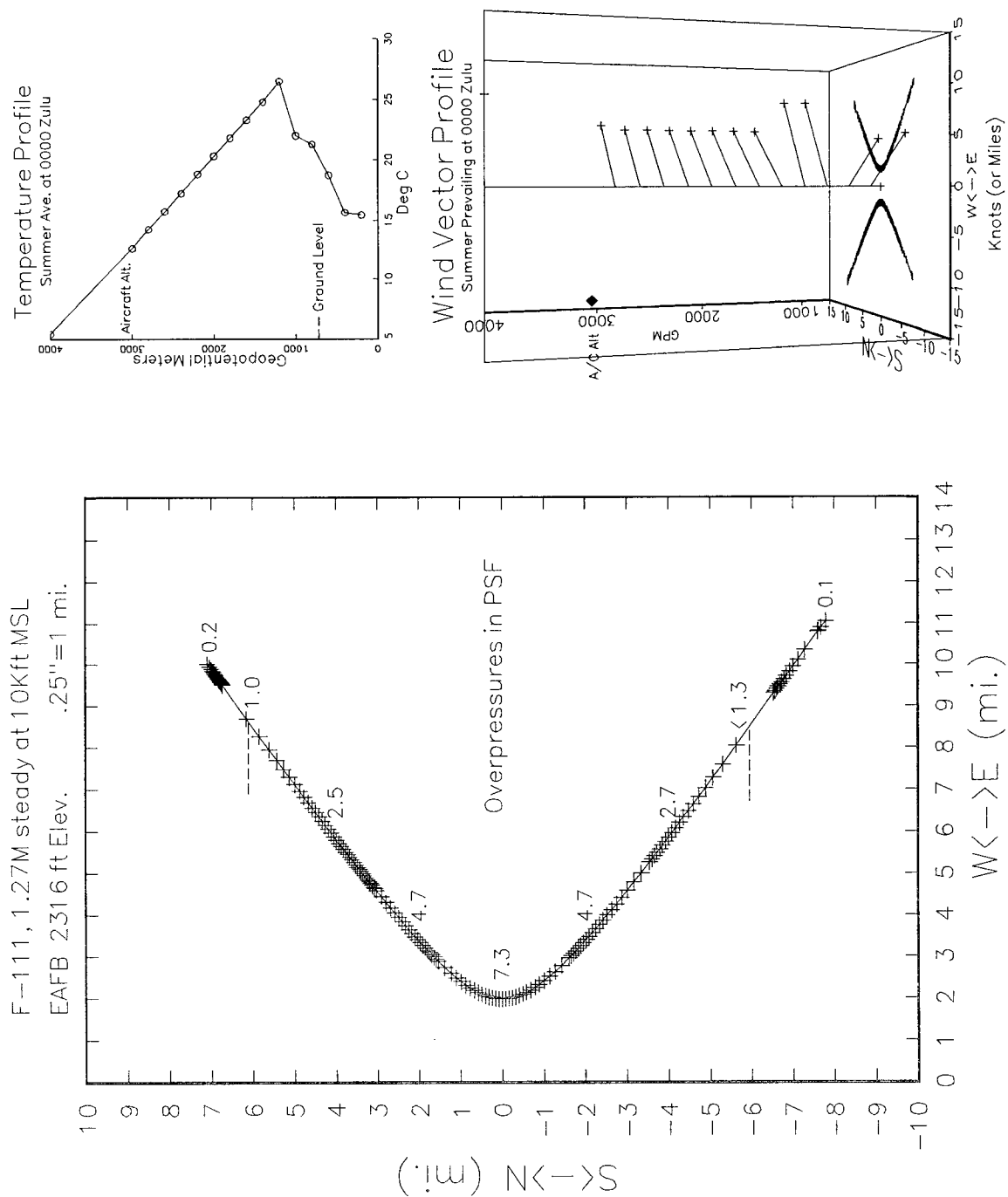


Figure 17. Average Summer Atmosphere at 0000 Zulu, Eastbound

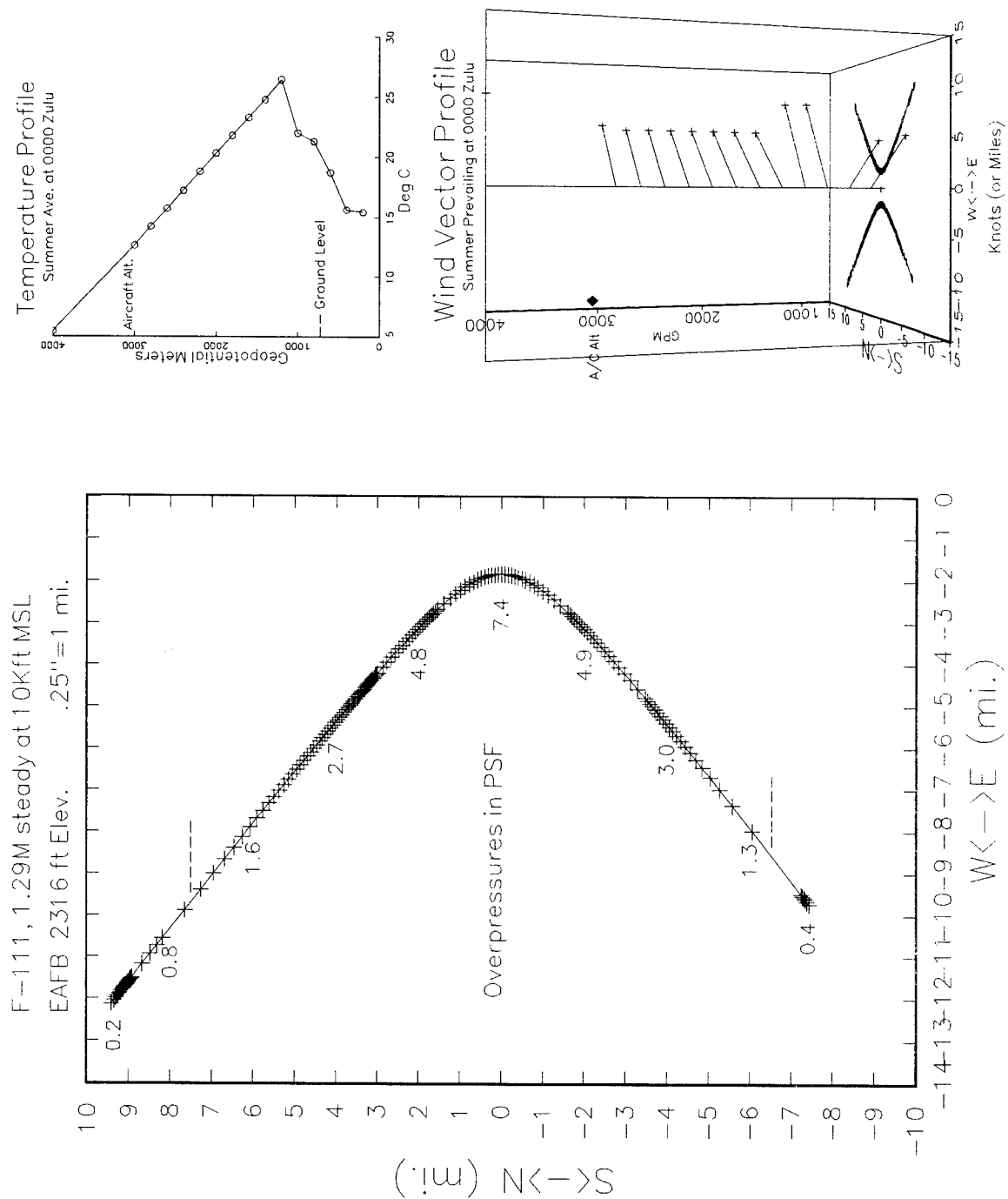


Figure 18. Average Summer Atmosphere at 0000 Zulu, Westbound

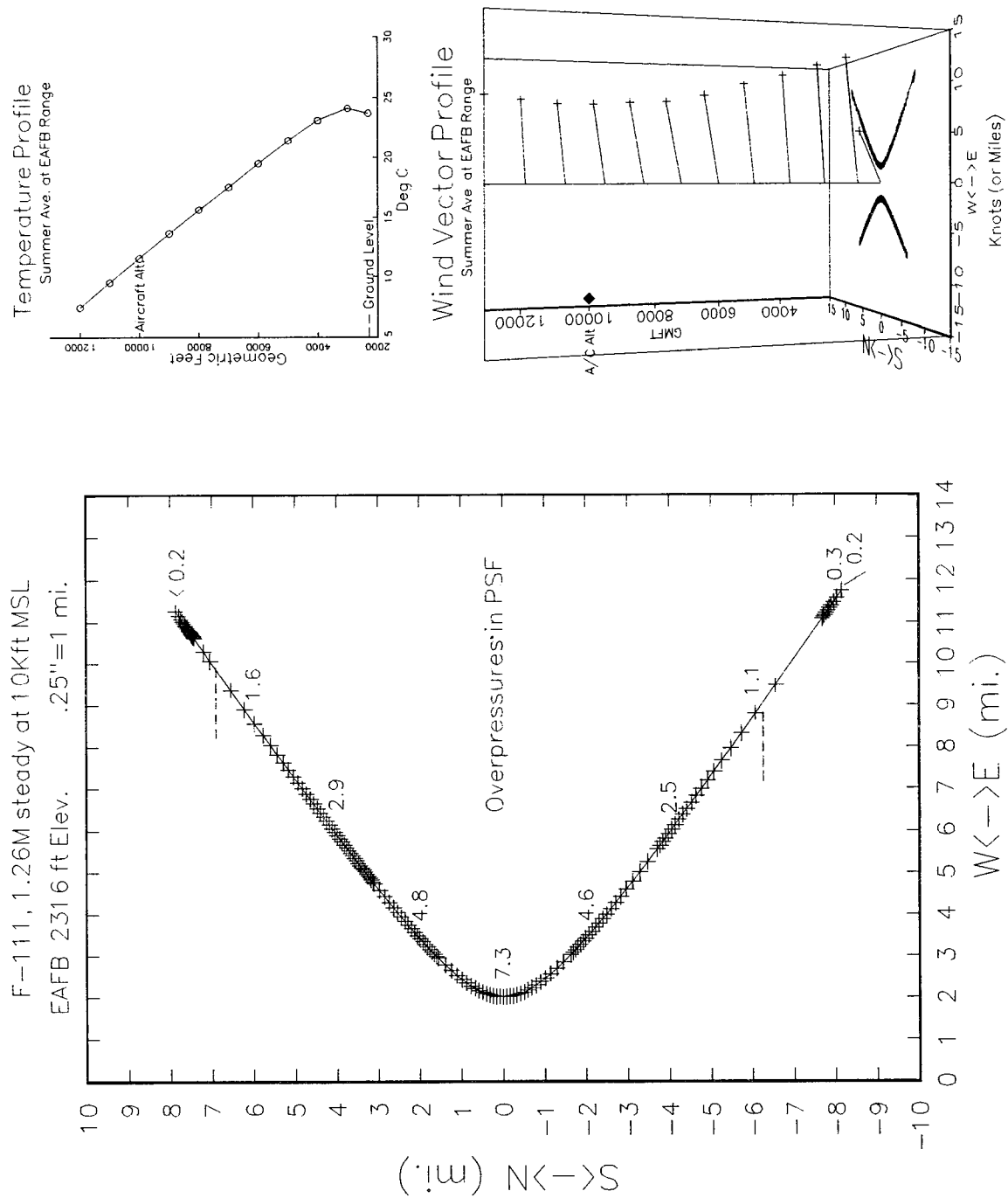


Figure 19. Average Summer Atmosphere at EAFB, Eastbound

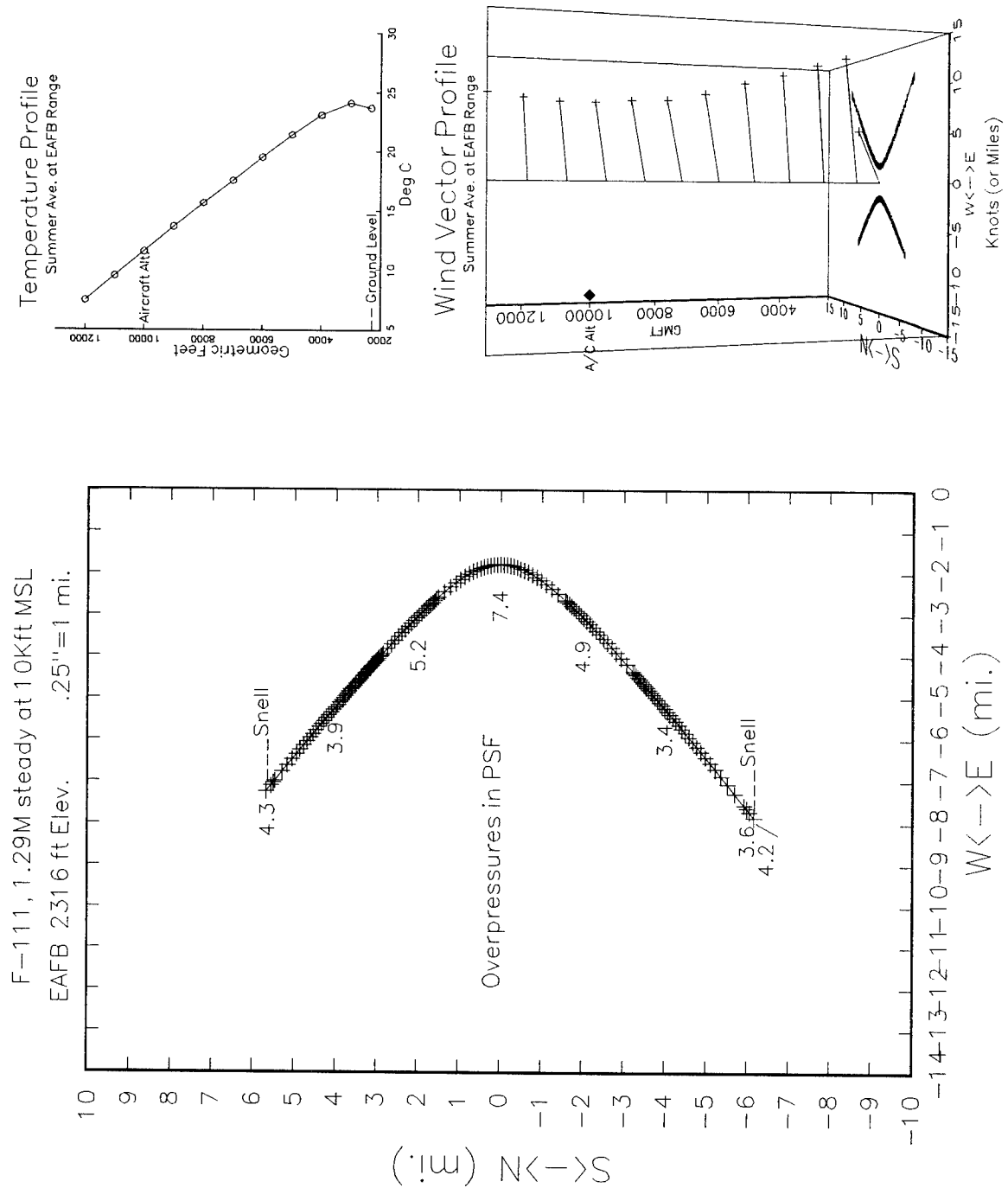


Figure 20. Average Summer Atmosphere at EAFB, Westbound

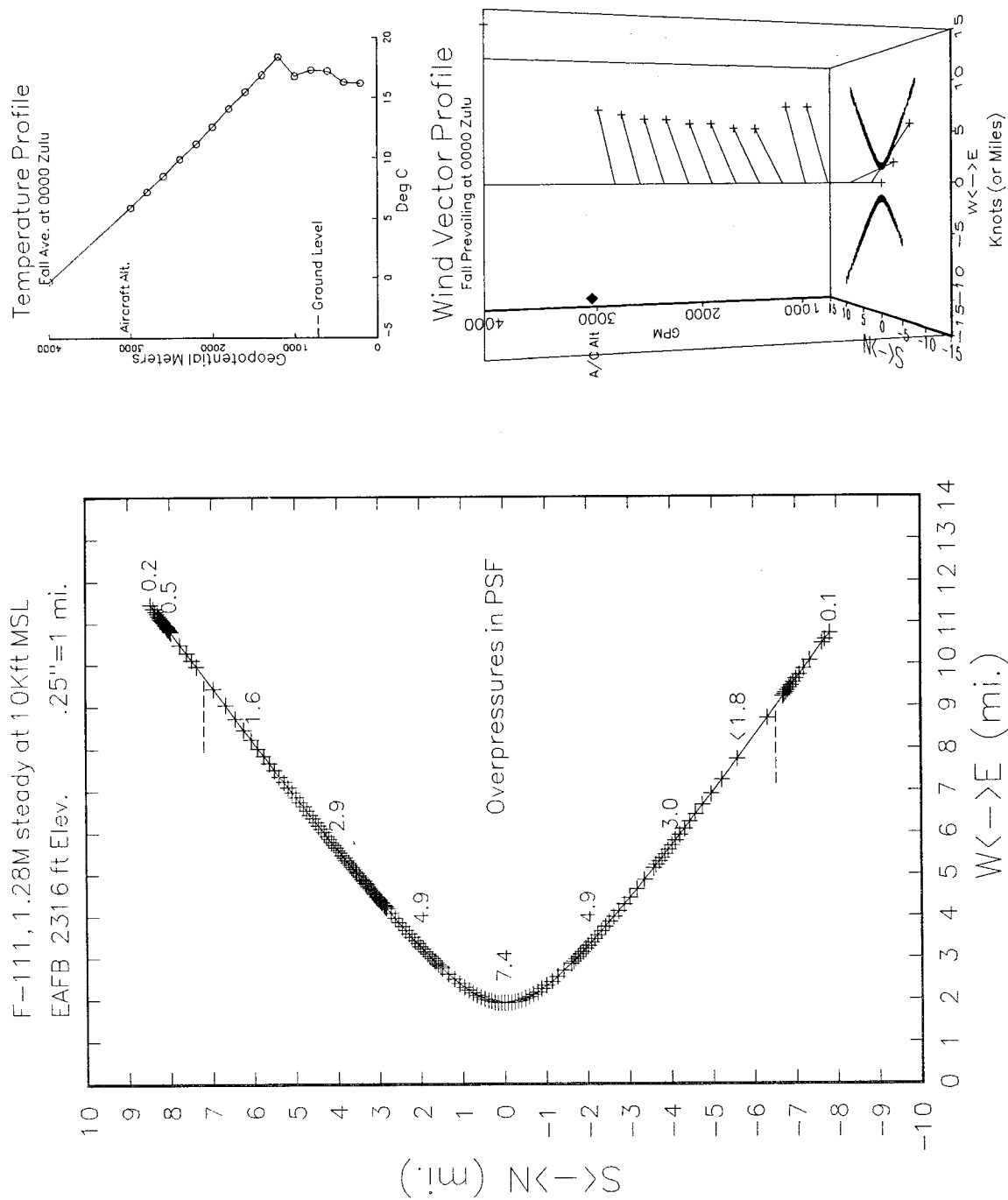


Figure 21. Average Fall Atmosphere at 0000 Zulu, Eastbound

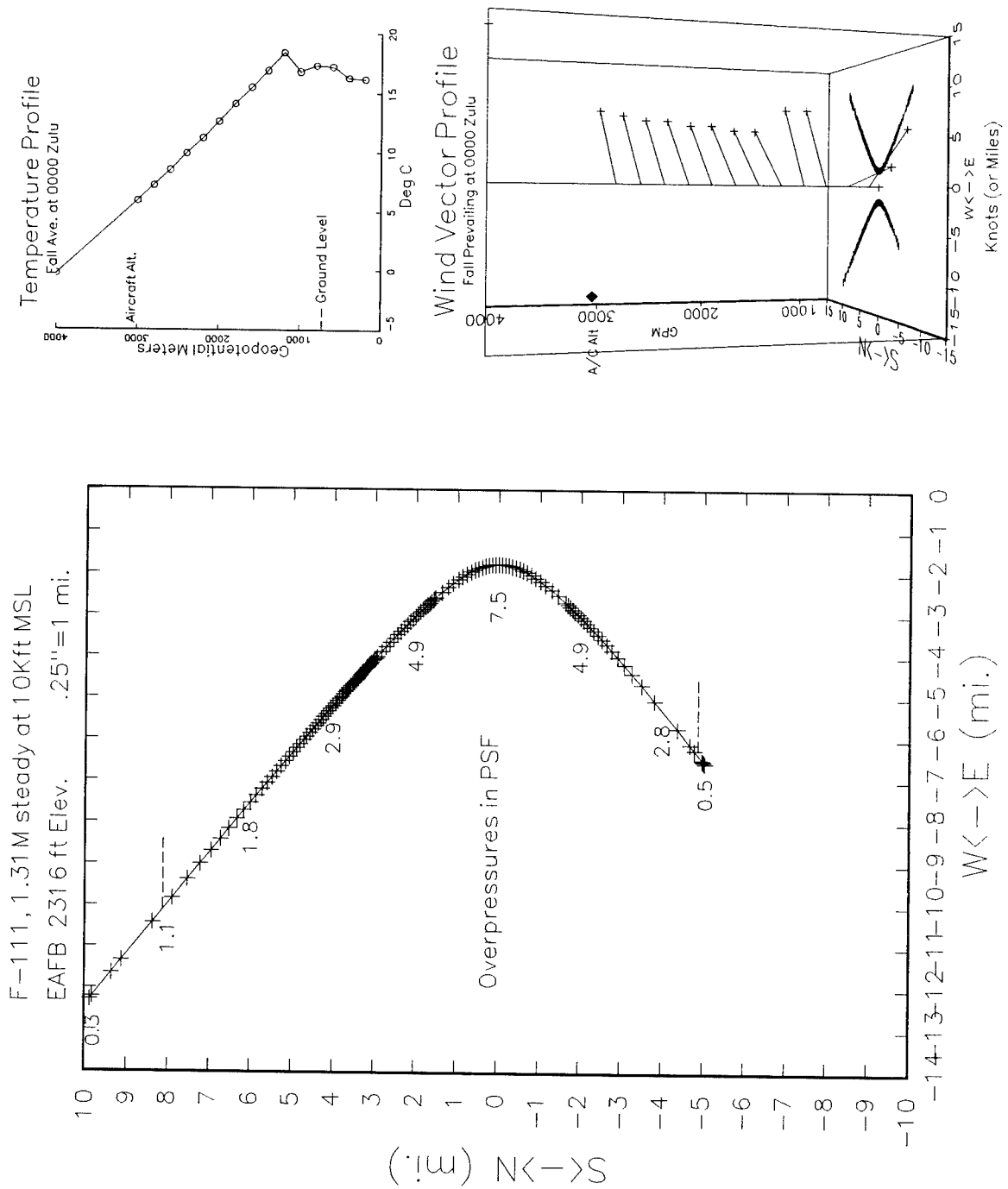


Figure 22. Average Fall Atmosphere at 0000 Zulu, Westbound

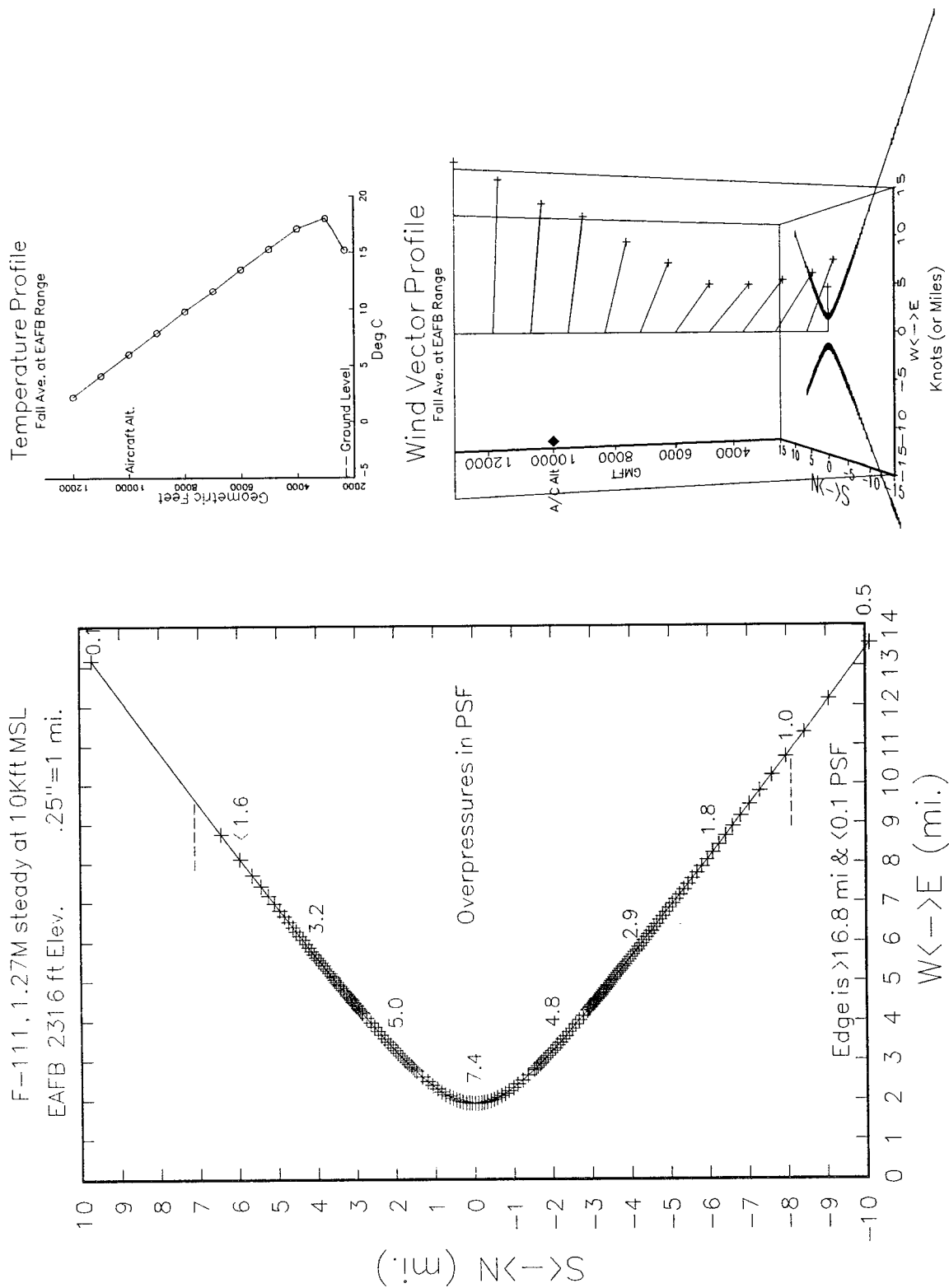


Figure 23. Average Fall Atmosphere at EAFB, Eastbound

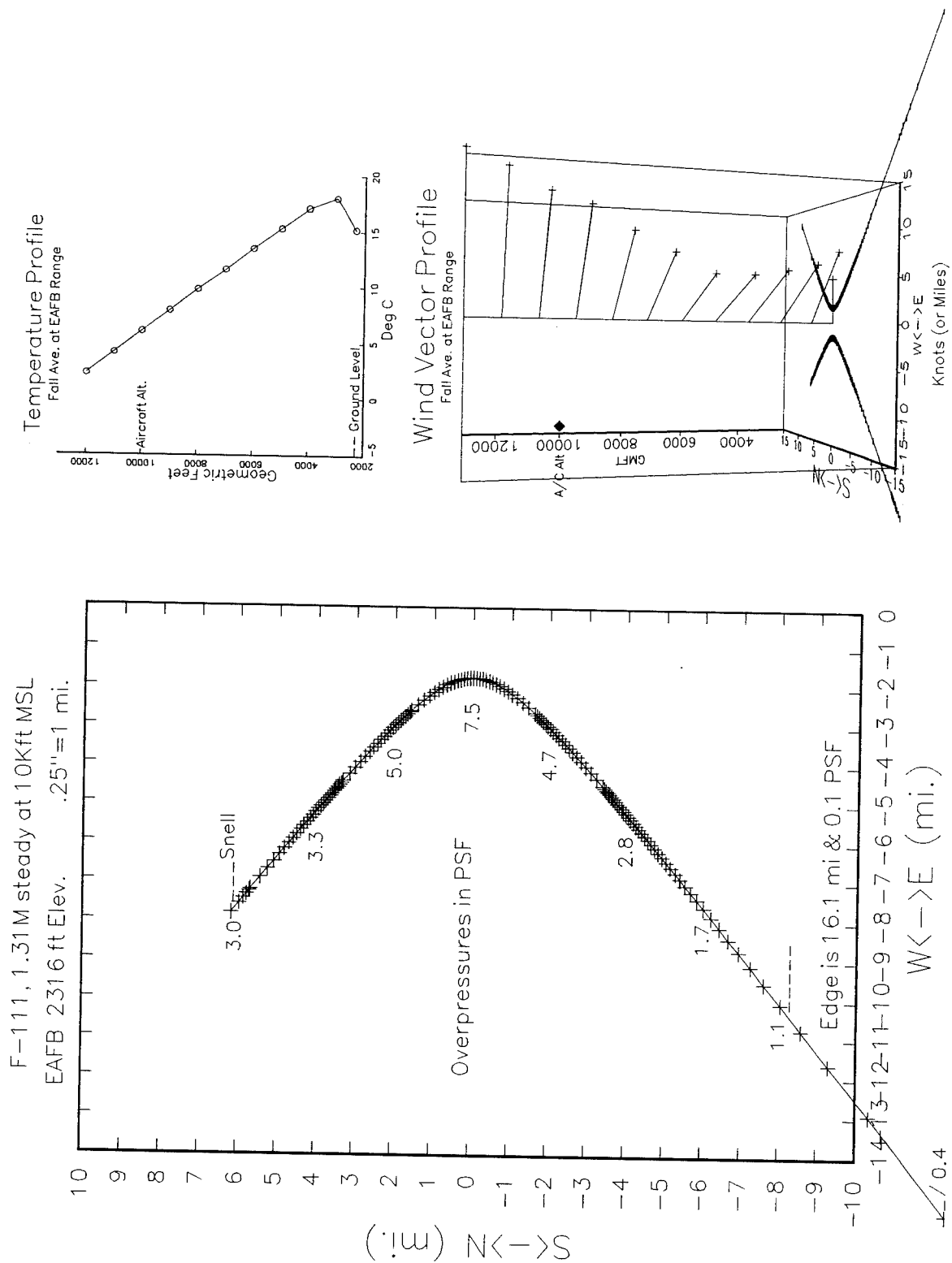


Figure 24. Average Fall Atmosphere at EAFB, Westbound



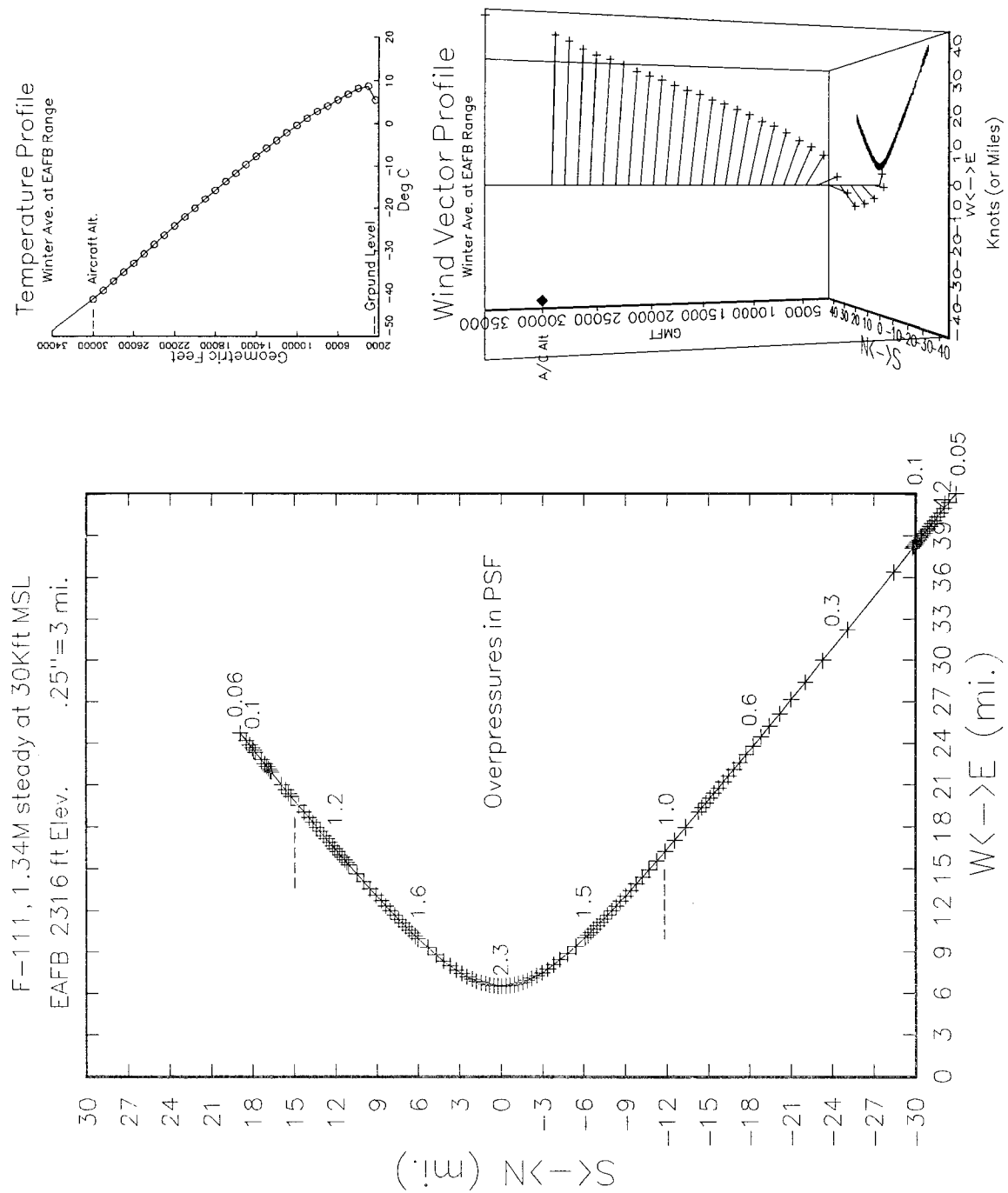


Figure 25. Average Winter Atmosphere at EAFB, Eastbound at 30 Kft MSL

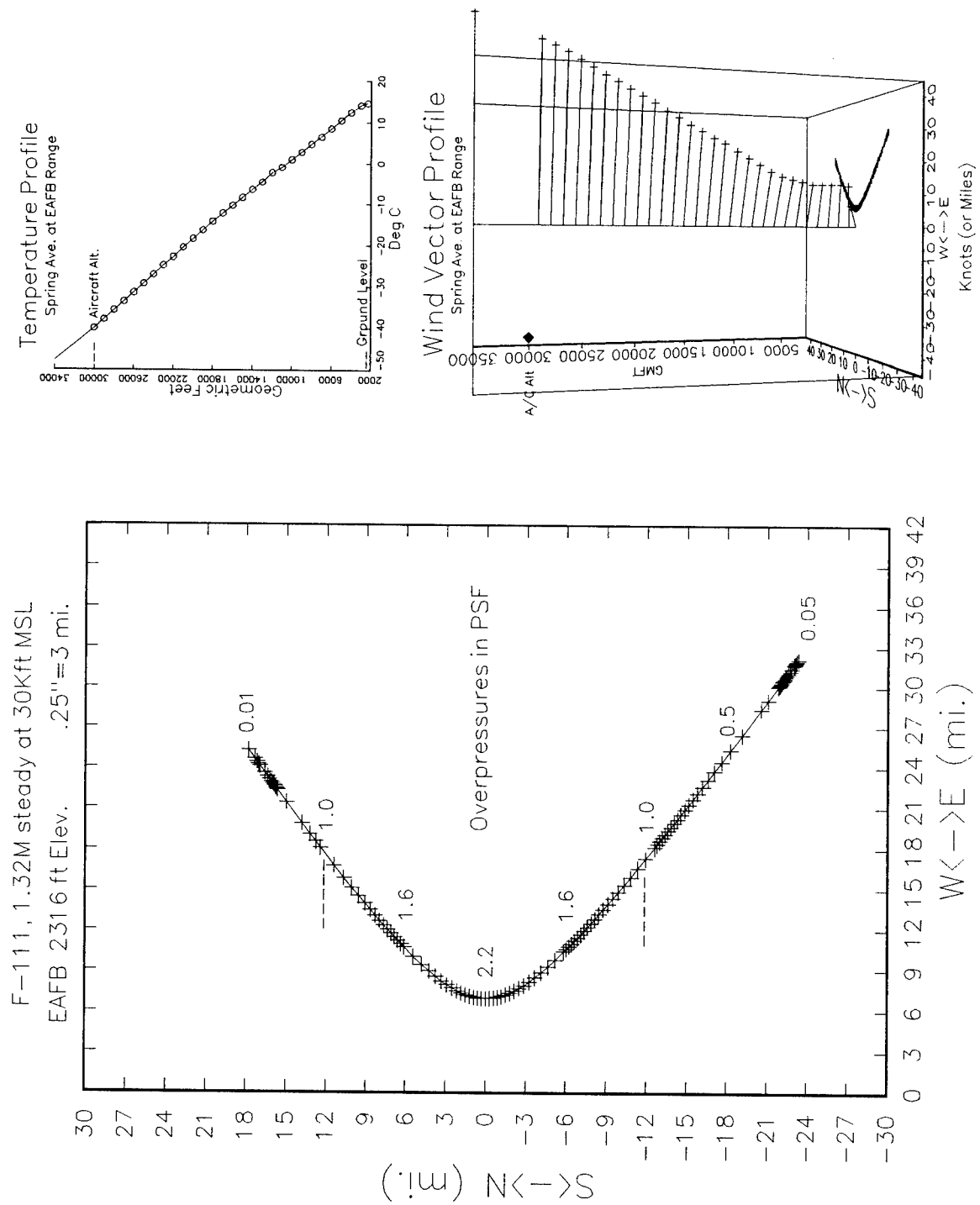


Figure 26. Average Spring Atmosphere at EAFB, Esatbound at 30 Kft MSL

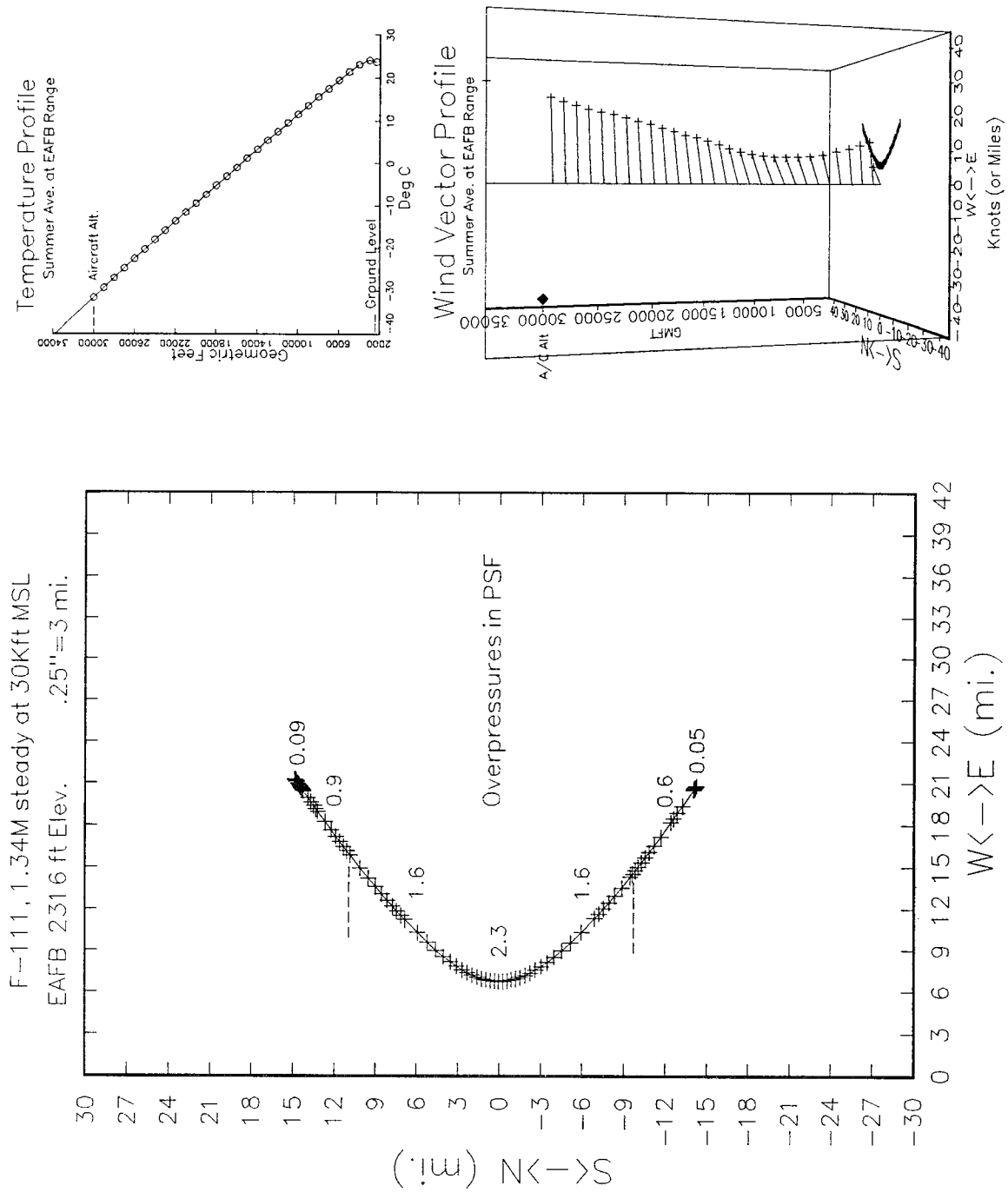


Figure 27. Average Summer Atmosphere at EAFB, Eastbound at 30 Kft MSL

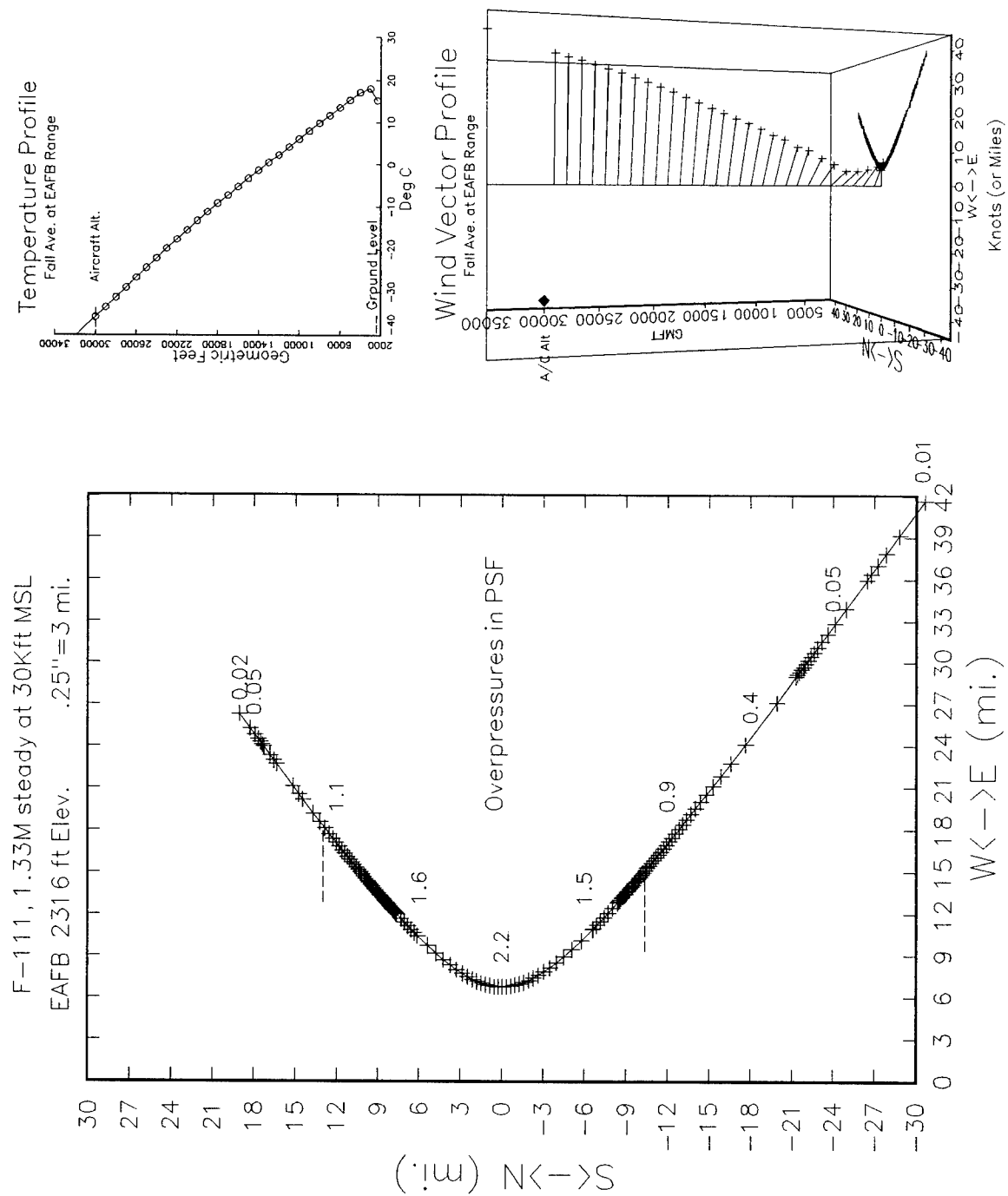


Figure 28. Average Fall Atmosphere at EAFB, Eastbound at 30 Kft MSL

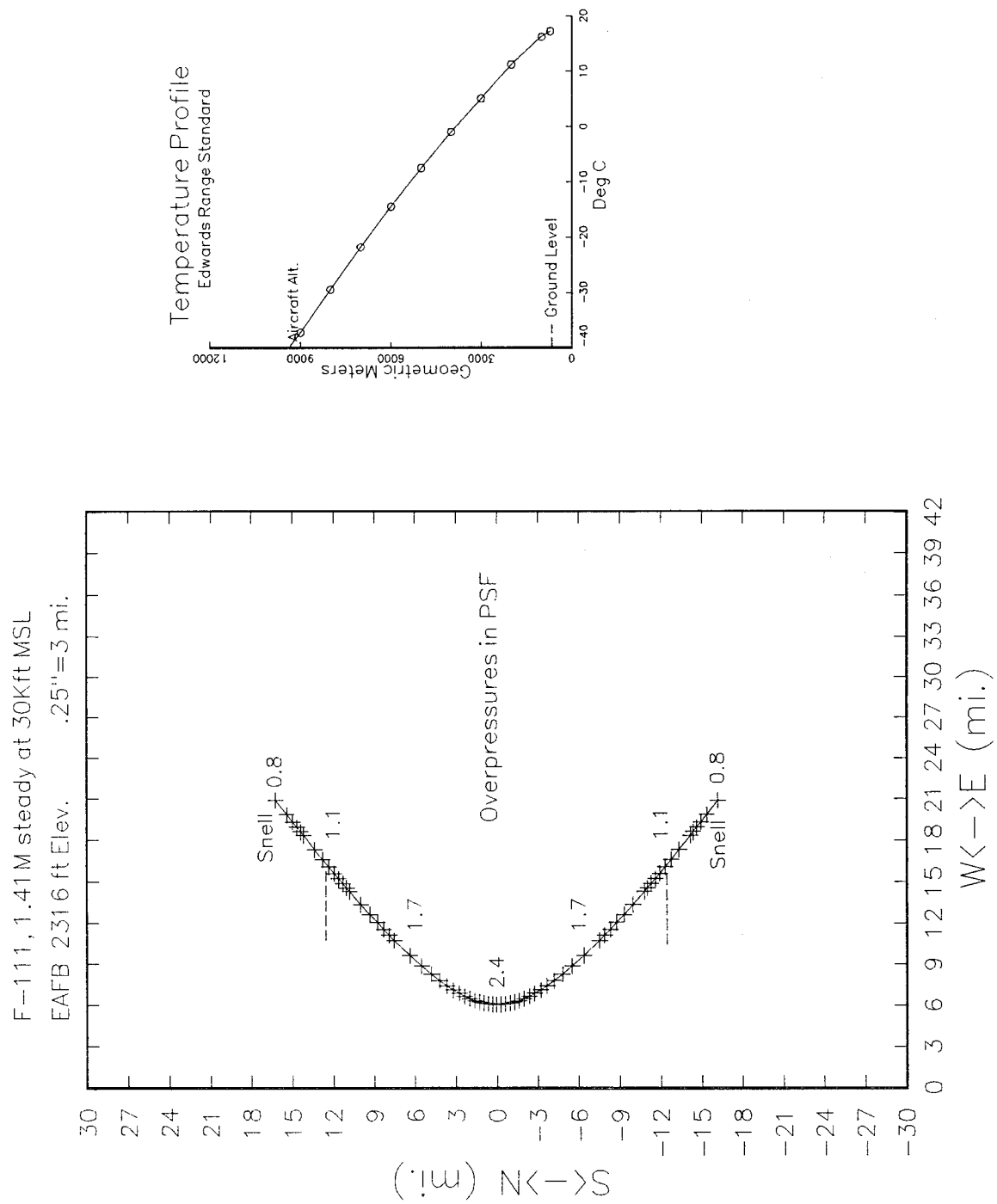


Figure 29. Edwards Range Standard Atmosphere, Eastbound at 30 Kft MSL

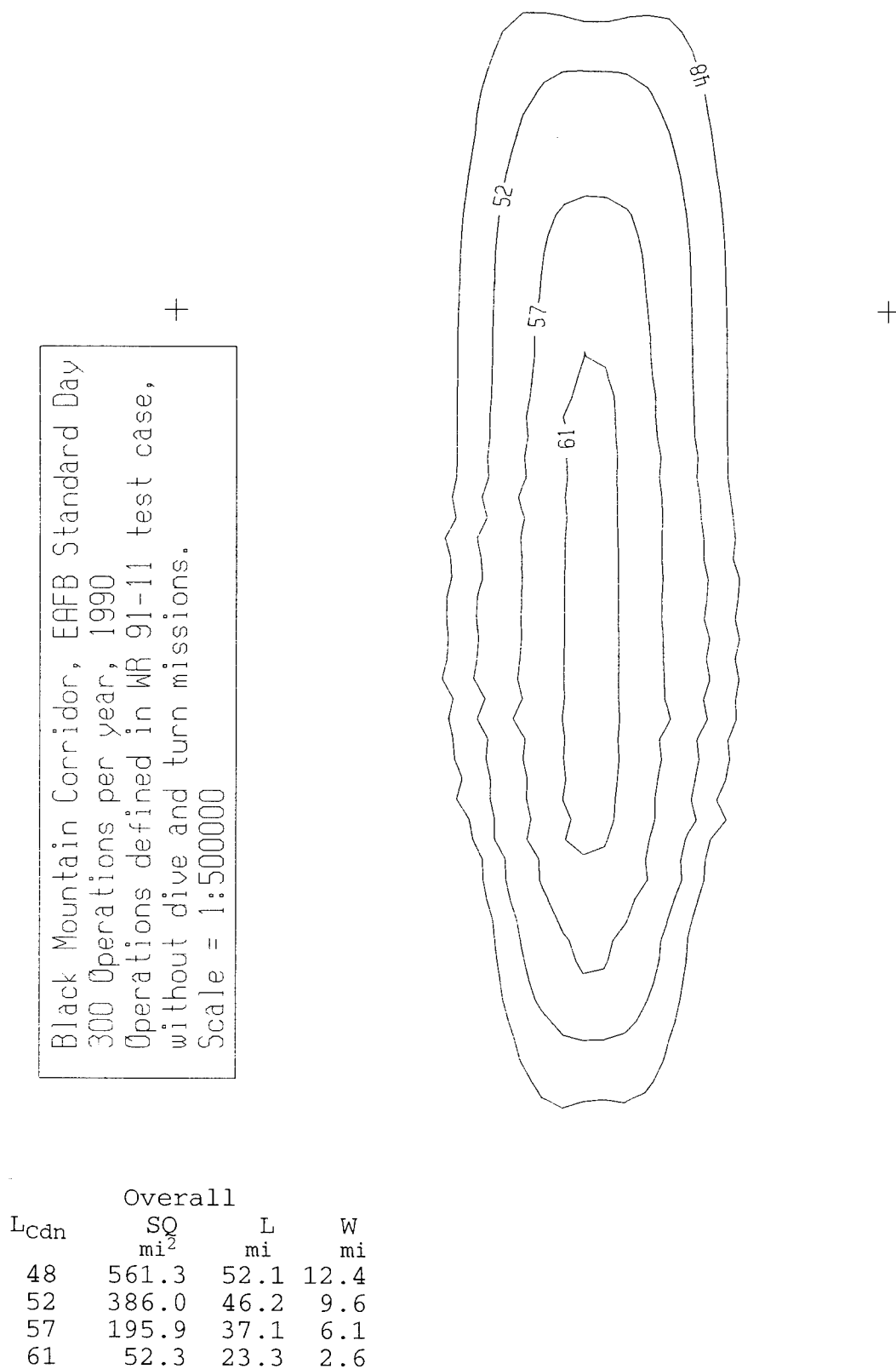
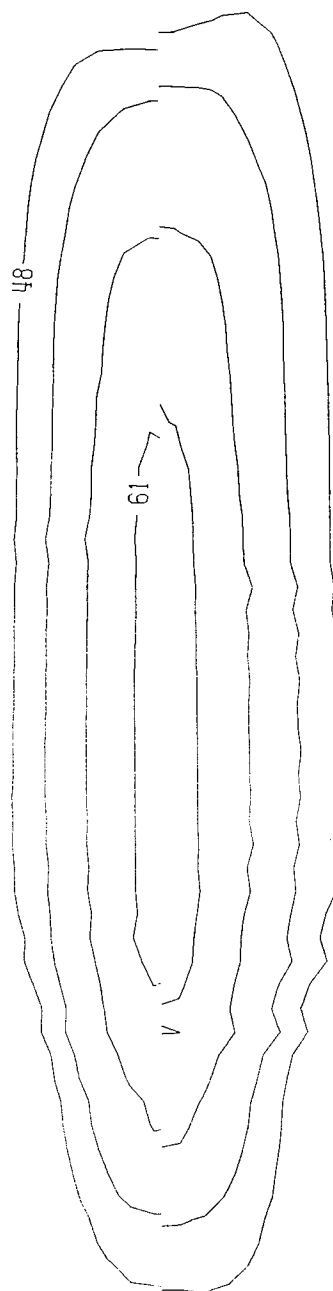


Figure 30. L<sub>Cdn</sub> Contour for Edwards AFB Standard (windless) Atmosphere.

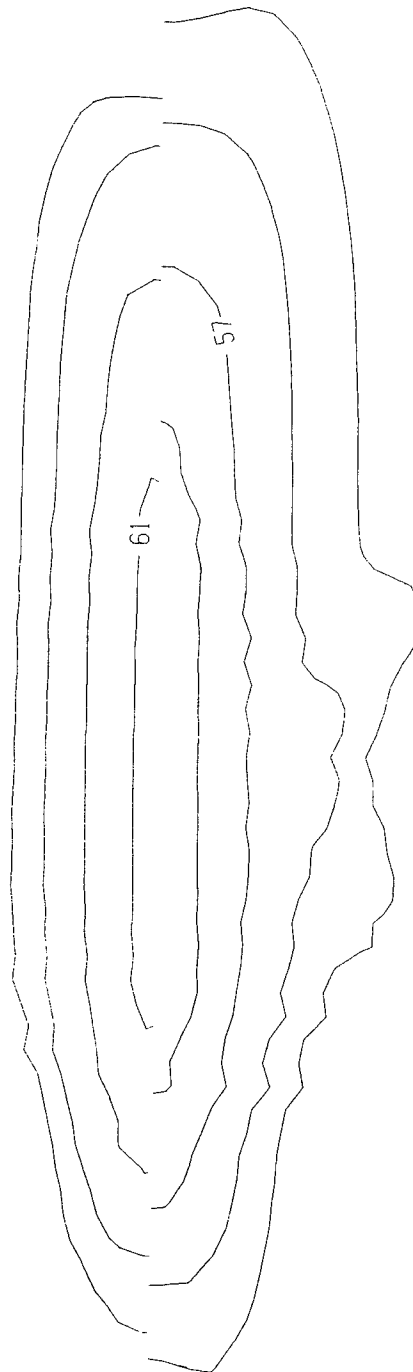
Black Mountain Corridor, Annual Weather  
 300 Operations per year, 1990  
 Operations defined in WR 91-11 test case,  
 without dive and turn missions.  
 Scale = 1:500000



L <sub>Cdn</sub>	Northbound			Southbound			W mi
	SQ <sub>N</sub> mi <sup>2</sup>	L <sub>N</sub> mi	W <sub>N</sub> mi	SQ <sub>S</sub> mi <sup>2</sup>	L <sub>S</sub> mi	W <sub>S</sub> mi	
48	484.1	50.7	5.5	593.5	52.9	6.4	11.9
52	338.1	45.6	4.2	405.9	46.6	5.0	9.2
57	172.9	36.5	2.7	206.9	37.7	3.1	5.8
61	41.3	22.7	1.0	58.6	23.9	1.4	2.4

Figure 31. L<sub>Cdn</sub> Contour for Edwards AFB Annual Average Atmosphere.

Black Mountain Corridor, Winter Weather  
 300 Operations per year, 1990  
 Operations defined in WR 91-11 test case,  
 without dive and turn missions.  
 Scale = 1:500000



L <sub>Cdn</sub>	Northbound			Southbound			
	SQ <sub>N</sub> mi <sup>2</sup>	L <sub>N</sub> mi	W <sub>N</sub> mi	SQ <sub>S</sub> mi <sup>2</sup>	L <sub>S</sub> mi	W <sub>S</sub> mi	W mi
48	468.1	50.7	5.3	777.5	55.6	8.0	13.3
52	328.5	45.2	4.2	468.3	47.3	5.7	9.9
57	169.8	36.5	2.7	227.6	38.5	3.4	6.1
61	38.3	22.3	1.0	80.8	26.6	1.7	2.7

Figure 32. L<sub>Cdn</sub> Contour for Edwards AFB Winter Average Atmosphere.



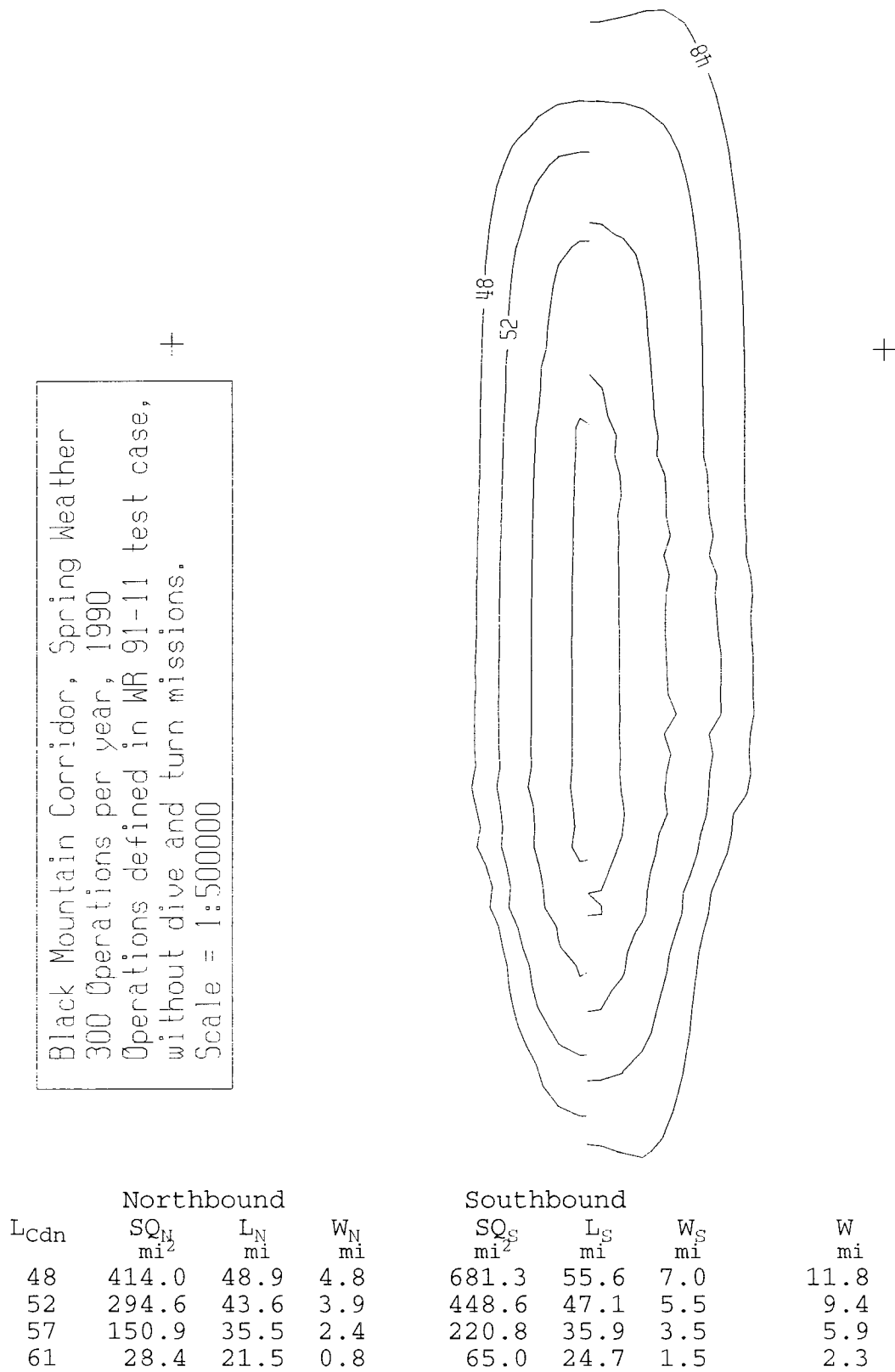


Figure 33.  $L_{Cdn}$  Contour for Edwards AFB Spring Average Atmosphere.

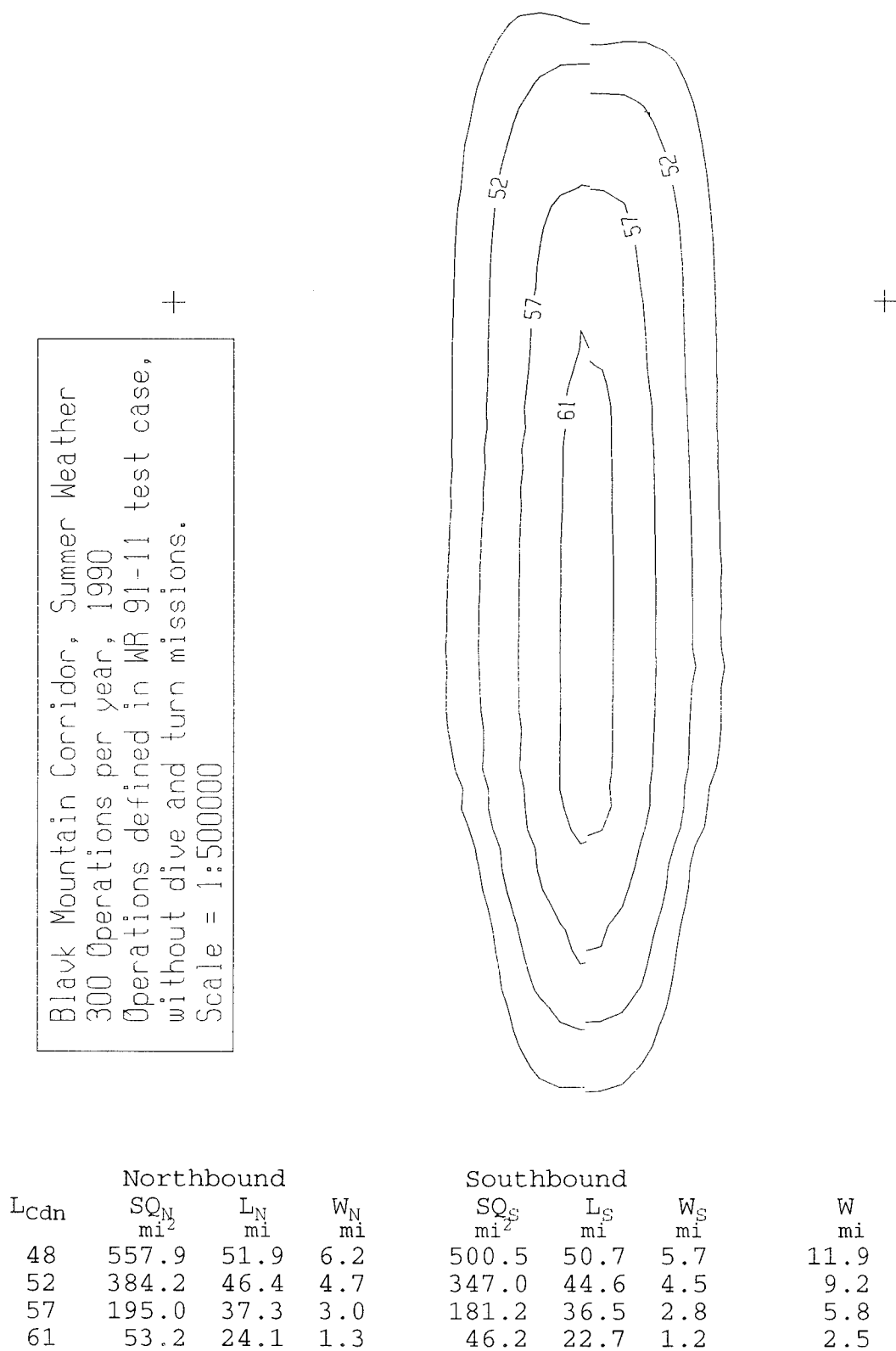
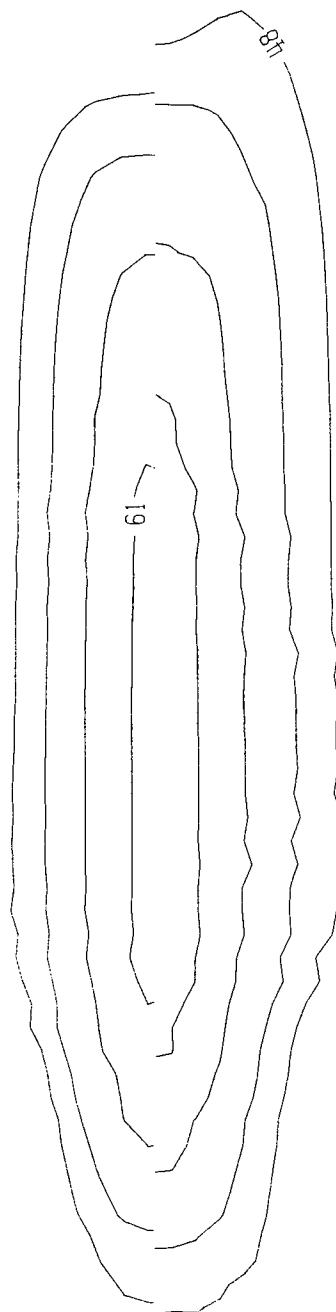


Figure 34.  $L_{cdn}$  Contour for Edwards AFB Summer Average Atmosphere.

Black Mountain Corridor, Fall Weather  
 300 Operations per year, 1990  
 Operations defined in WR 91-11 test case,  
 without dive and turn missions.  
 Scale = 1:500000



$L_{Cdn}$	Northbound			Southbound			$W$ mi
	$SQ_N$ mi <sup>2</sup>	$L_N$ mi	$W_N$ mi	$SQ_S$ mi <sup>2</sup>	$L_S$ mi	$W_S$ mi	
48	457.8	49.7	5.3	632.5	54.1	6.7	12.0
52	320.3	44.4	4.1	420.7	47.0	5.1	9.2
57	168.6	36.5	2.6	216.9	37.9	3.3	5.9
61	38.4	21.9	1.0	77.2	27.0	1.6	2.6

Figure 35.  $L_{Cdn}$  Contour for Edwards AFB Fall Average Atmosphere.

recent developmental work and it's existence is noted here only for completeness. Estimates of the 1 PSF overpressure ground impact locations were calculated to a lesser accuracy because the Phi sweep method could not be optimized accordingly.

## RESULTS

The objectives of this report required separate predictive analyses and a comparison of the results obtained from each. Single-event sonic boom predictions utilized greater theoretical detail and illustrated the effects due to average atmospheric refraction most clearly. Several measures of the lateral spreading and overpressures of sonic boom were investigated and the results presented in the following sections. Cumulative sonic boom exposure contours comparable to those routinely included in Environmental Impact Statements were generated to summarize the effect of a seasonally-varying atmosphere on long-term sonic boom predictions. Measures of lateral spreading and shifting were then calculated and compared relative to equivalent measures obtained from the detailed single-event propagation analysis.

### Propagation from 10,000 feet MSL

Figures 1 through 4 show the windless annual atmospheric profiles (U.S. Standard Day atm., Edwards Range Standard atm., NWS Regional Average atm., and EAFB Average atm.) and their respective sonic boom carpet predictions. Figures 5 through 8 incorporate the wind vector profiles into the averaged annual atmospheres and document the changes which then occur for aircraft flying East and West. Similar variations are to be expected for aircraft flying along different headings, which were not included in this study. In fact, the refractive effect would be somewhat more pronounced if the aircraft flew perpendicular to the prevailing wind. Figures 9 through 12 show the average winter atmospheric profiles and sonic boom predictions. The spring (Figures 13-16), summer (Figures 17-20) and fall (Figures 21-24) data are given in comparable format. Tables 1 through 3 summarize measures of the predicted lateral spreading of sonic booms, with the data re-grouped to facilitate comparisons. The data in Tables 1 through 3 concisely demonstrate the effect which seasonal changes in atmospheric wind vector and temperature gradients have on acoustic propagation.

All overpressures at the actual geometric cutoff were 0.5 PSF or less. For those atmospheres where Phi was artificially limited, the overpressures at the limit were 1.8 to 5.4 PSF (Figures 1-24). The Phi admittance criteria used in TRAPS was derived from Snell's Law by applying a linear estimate of the refractive effect of wind, much the same as in an earlier work by Onyeonwu<sup>8</sup>, but without including  $\Delta T$  as a refraction parameter. It is clear from this theoretical exercise that the artificial limitation placed on Phi in the application of the azimuthal ray sweep algorithm should be reconsidered. Artificial cutoff of the sonic boom carpet thus occurs frequently when the atmospheric

profile is dominated by temperature gradient refraction, such as in Figures 1 and 2.

Calculations were made to confirm that this problem occurred independent of altitude using predictions made under four different atmospheric conditions; U.S. Standard Day, Edwards Range Standard, Edwards annual and summer average atmospheres. Test cases were run at 20 Kft, 30 Kft, 40 Kft and 50 Kft MSL, but no results were plotted. These tests showed that the artificial cutoff was dependant only on the atmospheric profile used. Overpressures predicted at the artificial cutoff decreased with increasing altitude.

Table 1. Measures of the Predicted Lateral Spread of Sonic Boom for Annual Atmospheres at EAFB Sonic Boom Corridor.

Description	Fig.	Mach	Peak PSF	1 PSF			Cutoff		
				Distance N	S	Width (mi.)	Distance N	S	Width (mi.)
Windless									
US Std	1	1.32	7.5	>7.75	>7.75	>15.5	--	--	--
EAFB Std	2	1.29	7.7	>9.5	>9.5	>19.	--	--	--
Regional	3	1.29	7.4	8.25	8.25	16.5	9.6	9.6	19.2
EAFB Ave	4	1.30	7.4	9.75	9.75	19.5	11.1	11.1	22.2
Windy									
Regional E	5	1.28	7.4	6.75	5.75	12.5	8.1	7.2	15.3
Regional W	6	1.31	7.5	7.5	4.75	12.2	9.0	4.8	13.8
EAFB Ave E	7	1.27	7.3	8.	8.25	16.2	9.9	19.5	29.4
EAFB Ave W	8	1.32	7.5	>5.25	>8.25	>13.5	--	--	--

Table 2. Measures of the Predicted Lateral Spread of Sonic Boom for the Regional Average Seasonal Atmospheres at EAFB Sonic Boom Corridor.

Description	Fig.	Mach	Peak PSF	1 PSF			Cutoff		
				Distance N	S	Width (mi.)	Distance N	S	Width (mi.)
Eastbound									
Winter	9	1.29	7.6	5.	>8.	>13.	6.3	--	>14.3
Spring	13	1.29	7.5	6.	6.75	12.7	7.3	7.9	15.2
Summer	17	1.27	7.3	6.	6.	12.	7.1	7.8	14.9
Fall	21	1.28	7.4	7.25	6.5	13.7	8.4	7.8	16.2
Westbound									
Winter	10	1.32	7.4	7.5	7.5	15.	8.4	11.1	19.5
Spring	14	1.32	7.4	6.5	5.	11.5	8.3	5.2	13.5
Summer	18	1.29	7.4	7.5	6.5	14.	9.4	8.4	17.8
Fall	22	1.31	7.5	8.	4.75	12.7	9.9	5.0	14.9

Table 3. Measures of the Predicted Lateral Spread of Sonic Boom for the Edwards AFB Range Average Seasonal Atmospheres at EAFB Sonic Boom Corridor.

Description	Fig.	Mach	Peak PSF	1 PSF			Cutoff		
				Distance N	S	Width (mi.)	Distance N	S	Width (mi.)
Eastbound									
Winter	11	1.29	7.5	7.	11.	18.	8.7	15.6	24.3
Spring	15	1.28	7.3	7.25	8.25	15.5	9.4	12.5	21.9
Summer	19	1.26	7.3	7.	6.25	13.2	7.9	8.1	16.0

Fall	23	1.27	7.4	7.	8.	15.	9.7	>16.8	>26.5
Westbound									
Winter	12	1.33	7.4	7.5	7.5	15.	11.5	20.0	31.5
Spring	16	1.33	7.5	>4.5	>6.75	>11.2	--	--	--
Summer	20	1.29	7.4	>5.75	>6.25	>12.	--	--	--
Fall	24	1.31	7.5	>6.	8.25	14.2	--	16.1	>22.1

Note: ">" = greater than, "--" = TRAPS admittance limited.

The windy average atmospheres show a distinct North-South asymmetry of propagation which is due entirely to the seasonal prevailing wind. The refractive effect of the wind causes the sonic boom to spread asymmetrically (i.e. "shift") such that the 1 PSF level contour extends up to 3.25 miles further north than south for westbound aircraft. The EAFB Average climatology gives incomplete estimates of 1 PSF impacts for most westbound aircraft due to the artificial cut-off problem. The 1 PSF contour's lateral spread was likewise up to 3 miles further south than north for eastbound aircraft. It is further evident that the technique used to develop the atmospheric profiles had an impact on the sonic boom predictions derived from them.

Measures of sonic boom carpet widths and predicted overpressures provide supporting but less meaningful information about the extent of atmospheric effects. The single-event prediction of the 1 PSF sonic boom carpet width varies seasonally by 3.5 to 4.75 miles depending on the atmospheric profile model used. The predictions of higher amplitude boom overpressures appear symmetrical, but are in fact shifted in proportion to their respective lateral spreads. This occurred most noticeably in the winter and spring for eastbound aircraft where up to 1.7 PSF differences were noted at similar lateral offset distances, as shown in Figures 9 and 13. Measures of the lateral spreads of higher-amplitude booms were not analyzed for the single-event sonic boom model.

#### Propagation from 30,000 feet

Atmospheric refraction tends to influence acoustic propagation from low-altitude aircraft flights more strongly than that from higher altitudes. A further study was conducted to document the refractive effect on propagation from the same aircraft and Mach number operating at 30 Kft MSL. Of course, such predictions involved a significantly different part of the atmosphere, since the upper atmosphere is somewhat more predictable than the boundary layer. These simulations were done only for an eastbound aircraft using the Edwards Range Average seasonal atmospheres and the Edwards Range Standard (windless) atmosphere. The results were plotted in Figures 25 through 29 using a 3X larger scale, and summarized in Table 4.

These sonic boom predictions showed that the effect of wind vector gradient refraction is a complex function of altitude. The 1 PSF carpet width varied by a similar amount, which is proportionately less than the width's variation at lower altitude because the carpet was wider. This is consistent with the theory of refraction which predicts stronger effects at lower propagation angles. The results were also interesting in that the northern 1 PSF spread varied more than the southern 1 PSF spread, a reversal from the trends seen at 10 Kft. These higher altitude sonic booms were influenced more by

the seasonally varying geostrophic wind than the boundary layer wind vectors. The plots of wind vector profile associated with Figures 25 through 28 show the switch from boundary layer to geostrophic winds quite well.

The differences between low and high-altitude single-event predictions precluded any direct deductions regarding estimates of the cumulative effect of seasonal refraction on a number of different operations such as are conducted at EAFB. Further comparisons correlating single-event predictions to long-term average predictions are needed.

**Table 4.** Measures of the Predicted Lateral Spread of Sonic Boom for the Edwards AFB  
Range Average Seasonal Atmospheres and  
Standard Atmosphere for an  
Eastbound Aircraft.

Description	Fig.	Mach	Peak PSF	1 PSF		Width (mi.)	Cutoff		Width (mi.)
				Distance N	S		Distance N	S	
Eastbound Windy									
Winter	25	1.34	2.3	15.25	11.25	26.5	18.9	33.0	51.9
Spring	26	1.32	2.2	12.0	11.75	23.7	17.8	23.3	41.1
Summer	27	1.34	2.3	11.0	9.75	20.7	14.9	14.2	29.1
Fall	28	1.33	2.2	12.75	10.75	23.5	19.0	30.7	49.7
Standard	29	1.41	2.4	12.5	12.5	25.0	>16.2	>16.2	>32.4

#### Overpressures at 10,000 feet

The peak overpressure directly under the flight path showed only small variations (Tables 1, 2 and 3). Such variations are known to be due to differences in propagation distance, Mach number, atmospheric pressure, and atmospheric absorption. The propagation distance varied by less than 2% at either altitude studied due to refraction. The effective Mach number was influenced because TRAPS used a fixed transit time to traverse a fixed ground distance. Thus the wind and temperature in each atmosphere caused the effective Mach number to vary slightly (see Tables 1-3 and Figures 1-29). It was determined by multiple regression that the effective Mach number, atmospheric pressure at aircraft and ground heights, and atmospheric temperature at aircraft and ground heights had the strongest effect on resultant overpressure, respectively, for the 10 Kft flights. Basic atmospheric profile statistics are given in Table 5.

The relative humidity contributed only slightly to overpressure variation due to its influence on the virtual temperature. In theory, humidity is an important parameter in atmospheric absorption, particularly at higher frequencies. However, TRAPS89 didn't include the effects of atmospheric absorption<sup>7</sup>. This was evident in that classic "N" waves were predicted even for very long propagation distances when high-frequency absorption would cause the boom to be rounded.

**Table 5. Summary of Atmospheric Profile Statistics.**

Description	Figure Numbers	Aircraft Altitude			Ground Level		
		Press. mb	Temp. °C	Hum. %	Press. mb	Temp. °C	Hum. %
U.S. Std.	1	696.9	-4.8	~18	931.8	10.4	~39
Edwards Std.	2	713.2	5.1	~21	934.6	17.3	~42
Regional Ann.	3,5&6	709.5	5.1	21	935.4	15.5	42
Edwards Ann.	4,7&8	705.5	4.3	25	932.1	14.7	36
Regional Win.	9&10	706.9	-0.3	21	936.6	12.2	41
Edwards Win.	11&12	703.5	-0.5	24	935.3	5.5	37
Regional Spr.	13&14	706.9	1.9	21	935.2	12.7	48
Edwards Spr.	15&16	701.9	0.9	27	930.0	14.6	39
Regional Sum.	17&18	713.9	12.6	21	934.8	18.7	42
Edwards Sum.	19&20	709.3	11.5	22	929.9	23.7	32
Regional Fall	21&22	710.3	5.9	22	935.1	17.2	40
Edwards Fall	23&24	707.5	6.0	25	933.2	15.2	33

#### **$L_{Cdn}$ Contours for 1990 Operational Data**

The CORBOOM 1.01 cumulative exposure contour model used in this study calculates sonic boom exposures which are averaged out over a whole year. The impact of seasonally varying refractive atmospheres could only be assessed by calculating a cumulative sonic boom exposure which was averaged out over a season. The CORBOOM predicted contours did not require numerical adjustment if it was assumed that each season is 1/4 of a year and that 1/4 of the total number of operations were conducted in each season. This assumption effectively postulates that a seasonal reference metric such as  $L_{Cdns}$  should be used if seasonally varying environmental impacts are to be assessed. Under the assumption given,  $L_{Cdns}$  is numerically equal to  $L_{Cdn}$  and the seasonal variation of operations conducted was not a factor in the predicted results. Thus it was possible to limit the discussion to atmospheric effects only, which is important to maintaining a reasonable comparison to the single-event model predictions. Actual seasonal  $L_{Cdns}$  contour predictions would require knowledge of the actual number of operations in each season, which is not difficult to obtain or extrapolate.

The two atmospheric profile datasets studied using a single-event propagation model for comparison were evaluated for application in a long-term exposure calculation. The Edwards AFB Range average (EAFB Average) meteorological profiles were selected for use because (1) they did not exhibit the aberrant profile discontinuities seen in Figures 9 and 13 and (2) they were developed by the local meteorologists and thus were regarded as more acceptable for application at Edwards AFB. Neither meteorological average profile was ideal for problems of this type, but no advanced techniques which produce average acoustic refraction effects were available for study<sup>9</sup>.

The contours produced by CORBOOM are shown in Figures 30 through 35. It was necessary to splice together semi-contours which were generated for northbound and southbound acoustic propagation. The respective  $L_{Cdn}$  contour areas were calculated by CORBOOM and used to estimate the corridor widths. It was considered to be unreliable to simply measure scaled contour widths since they varied somewhat and the



corridor centerline could not be ascertained accurately. Each semi-contour's scaled east-to-west length could be measured consistently via:  $L_{N,S}(\text{mi}) = 7.89(\text{meas. inches})$ . The scaling factor 7.89 was derived from the figure's scale and the number of inches per mile. Each semi-contour length was scaled and then used to calculate northbound ( $W_N$ ) and southbound ( $W_S$ ) semi-widths via:  $W_N(\text{mi}) = 0.57SQ_N(\text{mi}^2)/L_N(\text{mi})$ . The correction factor 0.57 was used to account for the oval shape of the contours and the fact that only a semi-width was required. These measures and the overall widths ( $W = W_N + W_S$ ) were calculated for each of four contour levels and tabulated with their respective figures (Figures 30-35).

#### Comparison of Single-Event to Long-Term Propagation Measures

A direct comparison between single-event and long-term measures of sonic boom exposure width and lateral shift due to wind refraction was made. The EAFB Average atmospheric propagation measures for a single eastbound sortie was used for comparison to equivalent measures for the 48 and 61 dB  $L_{Cdn(s)}$  contours. Similar measures for the westbound sortie and for the EAFB Standard Day were unavailable due to the artificial cutoff problem found in TRAPS89. However, the prevalent number of supersonic operations were comparable eastbound sorties. The measures obtained from the predicted 52 and 57 dB  $L_{Cdn(s)}$  contours were not tabulated but were entirely consistent with the figures given in Table 6 below. Lateral shifts were defined to be half the difference between southbound and northbound distances (semi-widths) and were calculated via  $S = [W_S - W_N]/2$ . The lateral shift therefore represents the approximate distance in miles that the 1 PSF overpressure (exposure contour) generated by an aircraft is offset southward from its flight track (or cumulative centerline).

A calculation was made of the proportion (in %) of each measure with respect to a normalizing measure. The ratio (%W) of predicted corridor widths with respect to the EAFB Standard Day width was calculated. [The EAFB Average windless profile single-event width (19.5 mi) was substituted for the truncated EAFB Standard Day single-event width (> 19 mi) because the respective predictions were otherwise very similar but an actual value was needed to provide a consistent baseline measure for all comparisons to windless atmospheric predictions.] The proportion (%S) of the predicted lateral shifts with respect to their associated widths was calculated. This calculation allows an assessment of the extent to which the presence of a large number of dispersed sorties mitigates or exaggerates the effects of atmospheric refraction due to an average wind. The wind's effect on cumulative exposure contours was evidently stronger than for a single event exposure and effected the high-level contours proportionately as much as the low-level contours.

**Table 6. Comparison of Single-event to  $L_{Cdn}$  Contour Measures of the Asymmetry of Lateral Sonic Boom Propagation.**

L <sub>Cdn(s)</sub>	Eastbound 1 PSF				48 dB L <sub>Cdn(s)</sub>				61 dB			
	W	%W	S	%S	W	%W	S	%S	W	%W	S	
%S												
Windless:												
EAFB Standard	19.5	-	0	0	12.4	-	0	0	2.6	-	0	0
Windy:												
EAFB Average	16.2	83	.1	1	11.9	96	.5	4	2.4	92	.2	8
EAFB Winter	18.0	92	1.5	8	13.3	107	1.3	10	2.7	104	.3	11
EAFB Spring	15.5	79	.5	3	11.8	95	1.1	9	2.3	88	.3	13
EAFB Summer	13.2	68	-.4	-3	11.9	96	-.3	-3	2.5	96	-.05	-2
EAFB Fall	15.0	77	.5	3	12.0	97	.7	6	2.6	100	.3	12

## CONCLUSIONS

The noise generated by aircraft, whether supersonic or subsonic, is significantly influenced by acoustic refraction during propagation to the ground. This effect has been incorporated into single-event sonic boom models with considerable success. This report explored state-of-the-art methods to assess the effects of seasonally varying refractive atmospheres on cumulative sonic boom exposure models. The results were generalized to understand the relationship between single-event aircraft flight noise models and much more universally applied airbase environmental noise models, such as NOISEMAP. This generalization merely assumes that the overall refractive effect on long-term average acoustic exposure contours is unaltered by the aircraft's velocity.

The total land area impacted in the case examined here is not a significant issue for two reasons: (1) atmospheric refractive effects are dependant on the aircraft's altitude and the magnitude and direction of the wind vector, both of which could cause greater seasonally-varying impacts in airbase environments and (2) the land values and compatible uses are much less significant in the desert than in communities which surround many military airfields.

- The results obtained for a single-sortie acoustic propagation model are strongly indicative of, and comparable to, results derived from multiple dispersed sorties in long-term acoustic exposure models.
- Techniques for estimating acoustic refractive effects due to seasonal variations in the atmosphere exist and provide meaningful information about the impact on long-term average acoustic exposure contours.
- The impact of seasonally-varying prevailing winds equated to a shift of 3 to 13% of the impacted acoustic exposure contour's width, regardless of the level of the contour. The overall contour's width varied seasonally between 88 and 107% of it's annual average value.-- The effect calculated was due to the orthogonal wind component, and would necessarily be greater if the full wind vector were included, the wind vector were greater or if the aircraft's altitude were lower.

## RECOMMENDATIONS

### For planning purposes

In planning operational flight paths, the asymmetric propagation of sonic booms due to seasonal weather effects should be considered to minimize the potential for adverse community response.

### For research and development

Further study of seasonal variations in acoustic exposures should be undertaken to define a methodology and metrics for application to long-term Environmental Assessments. Techniques for characterizing a set of discrete atmospheric profiles with an atmospheric profile which correctly predicts an average propagated sound level<sup>9</sup> should be examined for application in annual or seasonal acoustic exposure prediction models.

A single-event sonic boom model should be developed which does not suffer from the limitations caused by the TRAPS Phi sweep algorithm. The Admittance Ellipse criteria needs to be re-examined and improvements made to the focus-finding algorithms.

A single-event sonic boom prediction model should be developed which correctly accounts for atmospheric absorption along the acoustic ray propagation path. Inclusion of atmospheric absorption would necessarily reduce the predicted overpressures at long range, bringing the predictions near cutoff at least somewhat closer to measurements.<sup>10,11</sup>

The BOOMFILE database<sup>10</sup> should be studied in comparison to the predictions made by a single-event sonic boom model which accepts as input the actual Rawinsonde launch records collected during the measurement study. The atmosphere showed little variation during the BOOMFILE measurement time frame, which will limit the conclusions which may be drawn. However, since TRAPS allows actual tracking input, some benefit may be anticipated in predicting sonic boom focuses and signatures.

## REFERENCES

1. Data Transmittal from 510 OSS/WE, 6 Jan 92, WU 72313415.
2. Letter Report from ASD/WE dated 17 Aug 90, WU 72313415.
3. U.S. Standard Atmosphere, 1976. NOAA/NASA/USAF Washington, D.C., Oct 1976.
4. Hot, Cold, and Annual Reference Atmospheres for Edwards Air Force Base, California (1975 Version). NASA TM X-64970.
5. Plotkin, Kenneth J., "CORBOOM Model for the Prediction of  $L_{Cdn}$  in Supersonic Flight Corridors", WR 91-11.
6. Lundberg, Wayne R., "Analysis of Measured Environmental Noise Levels: an Assessment of the Effects of Airbase Operational Model Variables on Predicted Noise Exposure Levels", AL-TR-1991-0097, page 50.
7. Taylor, Albion D., The TRAPS Sonic Boom Program, NOAA Technical Memorandum ERL ARL-87, July 1980.
8. Onyeonwu, R.O. "The Effects of Wind and Temperature Gradients on Sonic Boom Corridors" Inst. for Aerospace Studies, Univ. of Toronto, 1971.
9. L'Esperance, A., Gabillet, Y., Schroeder, H. "Outdoor Sound Propagation: Experimental Study of Atmospheric Turbulence and Simulation with FFP", Proceedings of INTER-NOISE 92, pp.139, 1992.
10. Lee, R.A., Downing, J.M. "Sonic Booms Produced by United States Air Force and United States Navy Aircraft: Measured Data", AL-TR-1991-0099, p 34.
11. Downing, J.M. "Lateral Spread of Sonic Boom Measurements from U.S. Air Force BOOMFILE Flight Tests", AL-TR-1992-0095.